

Modeling the autophagic effect in tumor growth: a cross diffusion model and its free boundary limit

Xu'an Dou*

Jian-Guo Liu[†]

Zhennan Zhou[‡]

December 22, 2024

Abstract

In this paper, we propose two macroscopic tumor growth models to incorporate and investigate the spatial effects of autophagy. The cells are classified into two phases: normal cells and autophagic cells, whose dynamics are also coupled with the nutrients. First, we construct a fluid mechanical model describing the evolution of cell densities, where the drift is determined by the negative gradient of the joint pressure, and the reaction terms manifest the unique mechanism of autophagy. Next, in the incompressible limit, such a cell density model naturally connects to a free boundary model, describing the geometric motion of the tumor region. Analyzing the free boundary model in a special case, we show that the ratio of the two phases of cells exponentially converges to a “well-mixed” limit. Within this “well-mixed” limit, we obtain an analytical solution of the free boundary model which indicates the exponential growth of the tumor size in the presence of autophagy in contrast to the linear growth without it. We also provide extensive numerical simulations to illustrate the properties of the tumor models and explore with specially designed experiments the effects of autophagy, such as the enhancement of survivability.

Keywords: Autophagy, Tumor growth, Cross-diffusion, Free boundary problem

Mathematics Subject Classification: 35Q92, 35R35, 76D27, 92-10, 92D25

1 Introduction

The growth mechanism of solid tumors, or living tissues in general, is one of the central research topics in many disciplines. The relevant studies from the aspects of mathematical modeling, analysis, numerical simulation, etc. have been active in the past few decades (e.g., [3, 15, 28, 33, 40]). Tumor growth can be influenced by many factors and mechanisms such as concentration of nutrients, spatial availability due to contact inhibition, chemical signals, mutation and so on.

In this paper, we focus on *autophagy*, which is also a crucial mechanism for tumor growth [21, 22, 27]. Since de Duve introduced the term “autophagy” in 1963, it has attracted many researchers to study its various aspects. Roughly speaking, autophagy is a catabolic process during which cells “eat” their own constituents, to maintain homeostasis and to adapt to stress. Autophagy has been recognized as a process of fundamental significance with connections to many topics such as health, cancer, microbial injection and neurodegeneration [19, 20, 30–32, 37, 41].

In contrast to the importance and popularity of autophagy, few mathematical models have been proposed to understand the mechanism from the perspective of cell population dynamics. As far as we know, [18] is the first to establish an ODE model for cell population dynamics with the effects of autophagy. Here we present a modified version of their model, while capturing the essence of the unique mechanism:

$$\begin{cases} \frac{dn_1}{dt} = G(c)n_1 - K_1(c)n_1 + K_2(c)n_2. \\ \frac{dn_2}{dt} = (G(c) - D)n_2 + K_1(c)n_1 - K_2(c)n_2. \\ \frac{dc}{dt} = -\lambda(t)(c - c_B(t)) - \psi(c)(n_1 + n_2) + an_2. \end{cases} \quad (1)$$

*School of Mathematics Science, Peking University, Beijing, 100871, China (dxa@pku.edu.cn)

[†]Department of Mathematics and Department of Physics, Duke University, Box 90320, Durham, NC27708, USA (jliu@phy.duke.edu).

[‡]Beijing International Center for Mathematical Research, Peking University, Beijing, 100871, China (zhennan@bicmr.pku.edu.cn).

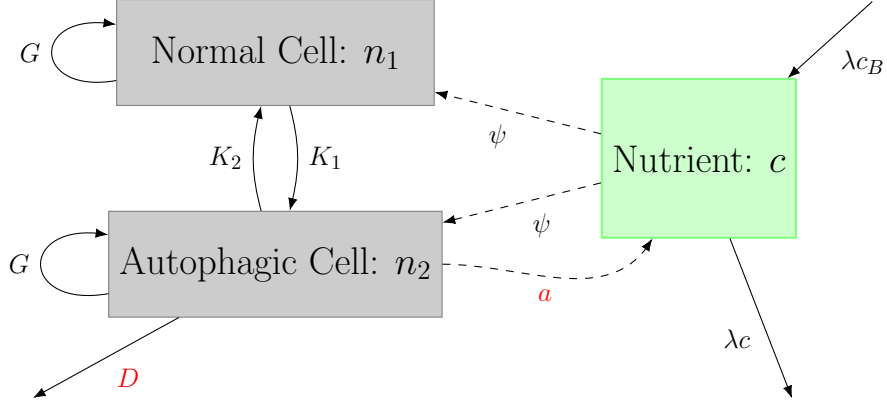


Figure 1: Illustration of the ODE model. The two gray squares denote the densities of normal cells n_1 and autophagic cells n_2 . And the green square denotes the nutrient concentration c . Normal cells change into autophagic cells with a transition rate K_1 . And autophagic cells change into normal cells with a transition rate K_2 . Normal cells and autophagic cells both grow with a net growth rate G . Dashed lines show the consumption or supply of nutrients by cells. Both normal cells and autophagic cells consume nutrients with a rate ψ . The key assumption is that autophagic cells will “kill” themselves with an extra death rate D to provide nutrients with a supply rate a . Nutrients are added with a rate λc_B and discharged with a rate λc .

In this ODE model (1), cells are classified into two phases: normal cells and autophagic cells. Their densities are n_1, n_2 while c denotes the concentration of nutrients. $G(c)$ is the net growth rate of normal cells, which could be understood as the birth rate minus the death rate. Autophagic cells have an extra death rate D due to the “self-eating” mechanism. Two types of cells can change from one type to another with transition rates $K_i(c)$, $i = 1, 2$. Both cells consume nutrients with the consumption rate $\psi(c)$, while autophagic cells provide nutrients with the supply rate a by degrading its own constituents. The nutrient solution is pumped in and out with the same rate $\lambda(t)$. Note that $\lambda(t)(c_B(t) - c)$ denotes the difference of nutrients between input flux and output flux, and thus it is the rate of change of the nutrient concentration due to the pumping process.

The key ingredient in this model is that while autophagic cells provide nutrients from the degradation of its own constituents with the nutrient supply rate a , the trade-off is an extra death rate D . We assume

$$D > 0, \quad a > 0, \quad (2)$$

are constants for simplicity.

The net growth rate for normal cells $G(c)$ increases with the concentration of nutrients. And the transition rates $K_1(c), K_2(c)$ are positive since autophagy is a reversible process. When the nutrient is deficient, autophagy is active and normal cells will change into autophagic cells faster. While when the nutrient is sufficient, autophagic cells will turn back to normal cells faster. Mathematically we have the following assumptions on G, K_1, K_2 :

$$G'(c) \geq 0, \quad K_1(c), K_2(c) > 0, \quad K_1'(c) \leq 0, K_2'(c) \geq 0. \quad (3)$$

For the consumption rate $\psi(c)$ we assume it is non-negative and increasing with c . When there is no nutrient the consumption rate shall be zero. Moreover, we assume there exists a critical nutrient concentration c_0 , such that $\psi(c_0) = a$. To summarize, we have the following assumption on the consumption rate $\psi(c)$:

$$\psi(0) = 0, \quad \psi'(c) > 0, \quad \exists c_0 > 0 \text{ s.t. } \psi(c_0) = a. \quad (4)$$

If $c > c_0$, then $\psi(c) > a$, which means the nutrient is sufficient enough that autophagic cells consume more nutrients than they supply. While when $0 < c < c_0$, $\psi(c) - a < 0$, which means autophagic cells supply more nutrients than they consume.

The ODE model (1) is based on the assumption that the spatial distributions of cells and nutrients are homogeneous. To our best knowledge, despite autophagy plays a crucial role in tumor growth, there is no spatial population model developed to understand its effect. The motivation of this paper is to study how autophagy influences the spatial growth of tumor. Hence, we propose and study a spatial model of tumor growth in the presence of autophagy.

Before we move on to spatial models, we remark that the effect of autophagy on the net growth rate is complicated. The introduction of the extra death rate D in (1) is a simplified assumption. In [18] they consider a different growth rate which can be interpreted as using $-\delta_2(\mu)n_2$ instead of $(G(c) - D)n_2$ in the second equation of (1). They assume $\delta_2(\mu)$ is the death rate of autophagic cells which depends on the ratio of normal cells in all cells $\mu = \frac{n_1}{n_1 + n_2}$. We stress that in both models the autophagic cells show a reduced net growth rate.

For how tumor grows in space, there have been numerous mathematical models in literature [28, 33, 40]. At the population level continuum models are widely used. Most continuum models fall into two categories: either they describe the densities of tumor from a fluid mechanics point of view [3, 39], or they treat the tumor as an expanding domain $\Omega(t)$ and describe its geometric motion, where free boundary problems arise [14, 15]. The connection between these two kinds of models has been established through the “incompressible limit” [29, 34].

First, we extend the ODE system (1) to a PDE system describing the evolution of cell densities, as a tumor growth model with the effects of autophagy. We denote the local density at position $x \in \mathbb{R}^d$, time $t \geq 0$ by $n_1(x, t)$ (or $n_2(x, t), c(x, t)$) instead of a homogeneous density $n_1(t)$ (or $n_2(t), c(t)$). The spatial motions of cells and nutrients are different. While for nutrients we assume they diffuse quickly, the spatial motion of cells is more complicated. We assume both kinds of cells are driven by a velocity field v . The velocity field v is induced by the local pressure $p(x, t)$ through Darcy’s law: $v = -\nabla p$ from a fluid mechanical view [34]. We connect the pressure to densities via the simplest constitutive law $p(x, t) = \frac{\gamma}{\gamma-1}(n_1(x, t) + n_2(x, t))^{\gamma-1}$ ($\gamma > 1$). Biologically the interpretation is that proliferating cells exert a pressure on their nearby cells, which pushes them to move. The full presentation of this PDE model is given in subsection 2.1.

Mathematically our assumptions on the spatial motion of cells lead to a porous-media type cross-diffusion system with reactions, of which a systematic treatment is still lacking in the current literature. In the absence of nutrients, existence is first established in [1, 2] with a non-vacuum assumption on initial data. Recently it is shown that well-posedness can be established without this assumption [5, 17, 38]. Moreover, the incompressible limit to a Heke-Shaw problem has been established [4] and the case when two kinds of cells have different mobilities has been studied [26].

The cross-diffusion system with reactions, which is also coupled with the dynamics of nutrients, is formidable for direct analysis. Such a cross-diffusion model can be interpreted as a cell density model, whose incompressible limit has been identified in previous work [4, 12, 34]. Heuristically, as $\gamma \rightarrow +\infty$, the cell density model becomes “incompressible” and converges to a free boundary model. The resulting free boundary problem is more tractable to obtain analytical results and is a useful approximation for the cell density model with large γ . There have been fruitful results studying the tumor growth in one-species cases with the help of the incompressible limit, for example traveling solutions [35], analytical solutions [24, 25] and numerical schemes [16, 23]. The incompressible limit in tumor growth model is first rigorously established in [34] and quite recently two-species cases [4, 13] and the case with nutrients [12] are studied, which are more relevant to our PDE model involving autophagy.

Next, we derive a free boundary model with a formal incompressible limit from the cell density model. Here we do not justify the limit rigorously but study the limited model directly. In the free boundary model, the cells are assumed incompressible and the tumor is described by an expanding domain $\Omega(t)$. The total density $n = n_1 + n_2$ inside $\Omega(t)$ is assumed to be a constant. And the pressure p and the concentration of nutrients c evolve as $\Omega(t)$ evolves. To describe the interplay of two kinds of cells, a density fraction $\mu(x, t)$ is introduced. $\mu(x, t)$ stands for the ratio of normal cells in all cells, corresponding to $\frac{n_1(x, t)}{n_1(x, t) + n_2(x, t)}$ in the cell density model. The formal derivation and full presentation of this model are given in subsection 2.2.

Free boundary models describing tumor consisting of different kinds of cells have been proposed directly, rather than from an incompressible limit, in literature around 2000. Ward and King [43, 44] consider models for living and dead cells. Pettet et al. [36] constructed a model for proliferating cells and quiescent cells. And a general free boundary framework was given by Friedman [14]. These multi-species free boundary models have attracted much mathematical interest for well-posedness [7, 10, 11], stationary solutions and stability [6, 8]. We note that in the presence of nutrients, the free boundary models are not exactly the incompressible limit of the cell density models when there is necrotic core [33, 35].

In summary, we construct two models to study spatial effects of autophagy in tumor growth: a compressible cell density model and an incompressible free boundary model. To investigate these two models, first we analyze the free boundary model. An interesting result here is that in a special case, we can obtain a clear asymptotic result for the density fraction μ : μ will converge to a spatial homogeneous constant state. We call this phenomenon the “well-mixed” limit. We obtain two results characterizing this limit: a uniform convergence result (Theorem 1) and convergence in the “ L^{2n} ($n \in \mathbb{N}^+$) norm” under a family of conditions (Theorem 2).

This “well-mixed” limit of density fraction μ allows us to further simplify the model and derive analytical solutions with a similar manner as in [24]. From the analytical solution we observe that when the nutrient provided by autophagy is sufficient, the tumor will expand exponentially in contrast to linear growth rate without autophagy in [24]. The essential reason behind the exponential growth is that when the extra nutrient supply rate a from autophagy has a bigger effect than the extra death rate D due to autophagy, the tumor can access to sufficient nutrients whatever big it is.

Then we carry out numerical simulations on the compressible cell density model, adapting the numerical scheme in [23]. By numerical experiments we first demonstrate the analytical results. Then we consider tumor in a container, corresponding to a PDE system with Neumann boundary condition, which is more similar to the ODE model. We perform numerical simulations on this model to study the effects of autophagy in more complicated scenarios.

Arrangement of this paper The rest of this paper is arranged as follows. We present the two models and discuss the assumptions on the free boundary model in Section 2. Under these assumptions, in Section 3 we analyze the free

boundary model and prove the “well-mixed” limit. Within the “well-mixed” limit, in Section 4 we obtain an analytical solution in a special case to further investigate the model. We also numerically demonstrate some analytical results. Finally, Section 5 is devoted to numerical simulations on the Neumann problem in more complicated settings.

2 Models and interpretations

In this section, we present the two models for tumor growth with autophagy: the compressible cell density model and the incompressible free boundary model. Moreover, the model assumptions are presented with detailed interpretations.

2.1 Compressible cell density model

We extend the ODE system (1) to involve spatial effects. We assume cells are driven by the negative gradient of pressure while nutrients diffuse quickly, which leads to the following PDE system:

$$\begin{cases} \frac{\partial n_1}{\partial t} - \nabla \cdot (n_1 \nabla p) = G(c)n_1 - K_1(c)n_1 + K_2(c)n_2, & x \in \mathbb{R}^d, t > 0. \\ \frac{\partial n_2}{\partial t} - \nabla \cdot (n_2 \nabla p) = (G(c) - D)n_2 + K_1(c)n_1 - K_2(c)n_2, & x \in \mathbb{R}^d, t > 0. \\ \epsilon \frac{\partial c}{\partial t} - \Delta c + \psi(c)(n_1 + n_2) = an_2, & x \in \mathbb{R}^d, t > 0. \\ c(x, t) \rightarrow c_B, \quad |x| \rightarrow \infty. \end{cases} \quad (5)$$

Here $n_1(x, t)$, $n_2(x, t)$ are local densities of two kinds of cells and $c(x, t)$ represents the local concentration of nutrients, at position $x \in \mathbb{R}^d$, time $t > 0$. As in the ODE model, $G(c)$ is the net growth rate of normal cells and $K_1(c), K_2(c)$ are transition rates with which two phases of cells change into each other. $\psi(c)$ is the consumption rate of nutrients. The key ingredient for autophagy in the ODE model is “inherited”: D is the extra death rate of autophagic cells and a is the nutrient supply rate from autophagy. The parameters satisfy (2)~(4) as in the ODE model.

For the spatial motion of cells, we take a fluid mechanical point of view. We assume they are driven by a velocity field which equals to the negative gradient of the pressure p (Darcy’s law) [34]. And the pressure arises from the mechanical contact between cells. Here we assume p is a power of total density $n = n_1 + n_2$, precisely:

$$p(x, t) = \frac{\gamma}{\gamma - 1} (n(x, t))^{\gamma - 1}, \quad n(x, t) := n_1(x, t) + n_2(x, t), \gamma > 1. \quad (6)$$

The choice (6) and Darcy’s law lead to porous-media type diffusion. Indeed if we add the first two equations in (5) and introduce the density fraction $\mu = \frac{n_1}{n_1 + n_2}$, then we obtain

$$\frac{\partial n}{\partial t} = \Delta(n^\gamma) + \mu G(c)n + (1 - \mu)(G(c) - D)n, \quad (7)$$

where $\Delta(n^\gamma)$ term arises.

For the spatial behavior of nutrients c , we assume they diffuse quickly. $\epsilon > 0$ is a parameter reflecting the time scale of the evolution of nutrients, which is usually smaller than cells. In the following we consider both the quasi-static case, i.e. $\epsilon = 0$, and the case $\epsilon = 1$. The boundary value c_B corresponds to the nutrients flux supplied by the environment. This system for nutrients has an important variant. When initially total density $n = n_1 + n_2$ has a compact support, then at least formally from the property of porous-media type diffusion (7), we deduce that $n(\cdot, t)$ has a compact support for every $t > 0$ (e.g., see section 4.2 in [33]). Thus $\Omega(t) := \{x : n(x, t) > 0\}$, the region occupied by tumor, is a bounded domain for all $t > 0$. Therefore we could use a different (and more realistic) model for nutrients:

$$\begin{cases} \epsilon \frac{\partial c}{\partial t} - \Delta c + \psi(c)(n_1 + n_2) = an_2, & x \in \Omega(t), \\ c = c_B, & x \notin \Omega(t). \\ \Omega(t) := \{x : n(x, t) > 0\}. \end{cases} \quad (8)$$

System (8) is used in the free boundary model.

To complete the system (5),(6), we should involve initial values of n_1, n_2 :

$$\begin{cases} n_1(x, 0) = n_1^0(x) \geq 0, \\ n_2(x, 0) = n_2^0(x) \geq 0, \end{cases} \quad (9)$$

and an initial value for nutrients c if $\epsilon > 0$.

Moreover, if we try to derive an equation for the density fraction $\mu = \frac{n_1}{n_1+n_2}$, with straightforward calculation we have (at least formally, since the definition of μ out the support of n is ambiguous)

$$\frac{\partial \mu}{\partial t} - (\nabla \mu) \cdot (\nabla p) = -\mu K_1(c) + (1 - \mu) K_2(c) + D\mu(1 - \mu), \quad (10)$$

which indicates the hyperbolic nature of the dynamics of two-species. This equation is used to characterize the two species dynamics instead the equations for n_1, n_2 in the free boundary model.

2.2 Incompressible free boundary model and assumptions

In this subsection, we derive and present the free boundary model. Then we give assumptions for the analysis in the next section.

2.2.1 Derivation of the free boundary model: a formal incompressible limit

We derive the free boundary model via a formal incompressible limit from the compressible cell density model (5). The formal derivation is quite standard [33, 34]. We refer to [29] for a rigorous analysis on the geometric motion of the limit Hele-Shaw problem in one species case.

To be concise we introduce two shorthand notations

$$G_1(c) := G(c), G_2(c) := G(c) - D, \quad (11)$$

which are the net growth rate of normal cells and autophagic cells, respectively.

First we multiply (7) with $\gamma n^{\gamma-2}$, which is the derivative of p with respect to the total density n , then we obtain

$$\frac{\partial p}{\partial t} - |\nabla p|^2 = (\gamma - 1)p(\Delta p + \mu G_1(c) + (1 - \mu)G_2(c)). \quad (12)$$

Formally let $\gamma \rightarrow \infty$ in (12), one obtains

$$p(\Delta p + \mu G_1(c) + (1 - \mu)G_2(c)) = 0. \quad (13)$$

Assuming p is bounded, as $\gamma \rightarrow \infty$ the relation of $p = \frac{\gamma}{\gamma-1} n^\gamma$ leads to

$$n(x, t) \begin{cases} = 1, & p(x, t) > 0. \\ \in [0, 1], & p(x, t) = 0. \end{cases} \quad (14)$$

To avoid the formation of necrotic core (c.f [9, 33, 35]), we assume the following weighted net growth rate is always non-negative:

$$\mu G_1 + (1 - \mu)G_2 \geq 0, \quad \forall x \in \mathbb{R}^d, t \geq 0. \quad (15)$$

Then for simplicity we assume the total density n is expanding as a characteristic function and we assume $\Omega(t)$ defined as in (8) satisfies:

$$\Omega(t) = \{x : n(x, t) > 0\} = \{x : n(x, t) = 1\} = \{x : p(x, t) > 0\} \quad (16)$$

Then from the equation of pressure p (13), we have

$$\begin{cases} -\Delta p = \mu G(c) + (1 - \mu)(G(c) - D), & x \in \Omega(t), \\ p = 0, & x \in \partial\Omega(t), \end{cases}$$

where in the first equation we substitutes the definition of G_1, G_2 in (11).

Since $n \equiv 1$ in $\Omega(t)$, we have $n_1 = n\mu = \mu, n_2 = n(1 - \mu) = 1 - \mu$. Thus, from (8) we have

$$\begin{cases} \epsilon \frac{\partial c}{\partial t} - \Delta c + \psi(c) = (1 - \mu)a, & x \in \Omega(t), \\ c = c_B, & x \in \partial\Omega(t). \end{cases}$$

For simplicity, in the free boundary model we focus on the quasi-static case: $\epsilon = 0$. We formally think the evolution of density fraction μ still satisfies (18) for $x \in \Omega(t)$ after taking the limit.

The last but subtlest component of the model is the evolution of $\Omega(t)$. We formally think the evolution of $\Omega(t)$ is determined by the motion of its boundary $\partial\Omega(t)$. And the moving speed of $\partial\Omega(t)$ is still determined by Darcy's law. The moving speed in the normal direction satisfies:

$$V_n = -\nabla p \cdot \mathbf{n}, \quad x \in \partial\Omega(t).$$

where \mathbf{n} is the outer normal direction of $\Omega(t)$.

2.2.2 Model and assumptions

To summarize, the free boundary model consists of 4 components: the time-dependent domain $\Omega(t)$, the pressure p which determines the moving speed of $\partial\Omega(t)$, nutrients c and the density fraction (of normal cells) μ for two-cells dynamics, which corresponds to $\frac{n_1}{n_1+n_2}$ in the compressible model. If $\mu(x, t) = 1$, it means locally all cells are normal cells. If $\mu(x, t) = 0$, it means locally all cells are autophagic cells.

Initially we shall specify a domain $\Omega(0)$ and an initial value for μ , $\mu(x, 0) = \mu_0(x)$ which is a function in $\Omega(0)$. Since μ_0 is the density fraction, it should take values in $[0, 1]$, i.e.,

$$\mu(x, 0) = \mu_0(x), \quad \mu_0(x) \in [0, 1], \quad x \in \Omega(0). \quad (17)$$

As time evolves, the density fraction μ satisfies a reaction-convection equation on a time-dependent domain while pressure p and nutrient c solves two elliptic equations for each time $t \geq 0$.

$$\frac{\partial \mu}{\partial t} - (\nabla \mu) \cdot (\nabla p) = -\mu K_1(c) + (1 - \mu) K_2(c) + D\mu(1 - \mu), \quad x \in \Omega(t). \quad (18)$$

$$\begin{cases} -\Delta p = \mu G(c) + (1 - \mu)(G(c) - D), & x \in \Omega(t), \\ p = 0, & x \in \partial\Omega(t). \end{cases} \quad (19)$$

$$\begin{cases} -\Delta c + \psi(c) = (1 - \mu)a, & x \in \Omega(t), \\ c = c_B, & x \in \partial\Omega(t). \end{cases} \quad (20)$$

The evolution of $\Omega(t)$ is determined by the motion of its boundary $\partial\Omega(t)$. Same as the compressible model, the moving speed of boundary is governed by the negative gradient of pressure (Darcy's law). Precisely, the moving speed in normal direction is

$$V_n = -\nabla p \cdot \mathbf{n}, \quad x \in \Omega(t). \quad (21)$$

As we will show in Proposition 1 in Section 3, under the Assumption 1 below, $V_n = -\nabla p \cdot \mathbf{n} > 0$ thus we do not need a boundary condition for the hyperbolic equation (18).

Last but not least, we impose the following assumption, which is inherited from (15) in the formal derivation.

Assumption 1. For $T > 0$, the weighted net growth rate $\mu G + (1 - \mu)(G - D)$ is non-negative, i.e.,

$$\mu(x, t)G(c(x, t)) + (1 - \mu(x, t))(G(c(x, t)) - D) \geq 0,$$

for all $x \in \Omega(t)$, $0 \leq t < T$. And for every $t \geq 0$ there exists at least one point $x \in \Omega(t)$ such that the strict inequality holds.

Assumption 1 allows the net growth rate of autophagic cells $G(c) - D$ to be negative, but assumes the nutrient is sufficient enough such that the weighted net growth rate is non-negative at every point in tumor. This is important for the connection between the free boundary system (17)~(21), which is already closed itself, and the limit problem of the compressible model (5).

Note that if Assumption 1 is true, then by maximum principle on nutrient depletion yields that $p(x, t) > 0$, for all $x \in \Omega(t)$. This rules out the formation of the necrotic core inside $\Omega(t)$, the case when the total density n decays to be less than 1 and pressure p becomes zero (see section 7.3 in [33]). Biologically, necrotic core means dead cells form a core in the tumor region due to the lack of nutrients [9, 35]. We numerically simulate the compressible cell density model to study the case when nutrient is not sufficient and the necrotic core is formed in Section 5.

Besides, we assume the following regularity of solutions for the analysis in next section.

Assumption 2. For $T > 0$, we have

1. $\Omega(t)$ is a bounded and simple-connected domain with smooth boundary for all $t \in (0, T)$. And the moving speed of boundary satisfies (21), that is, there exists a parameterization of the boundary $\Omega(t)$: $x(t, \alpha)$, $\alpha \in [0, 1]$, which satisfies

$$\frac{d}{dt}x(t, \alpha) = -\nabla p(x(t, \alpha), t), \quad x(t, 0) = x(t, 1).$$

for all $t \in (0, T)$, $\alpha \in [0, 1]$.

2. Let $Q_T = \{(x, t), x \in \overline{\Omega(t)}, t \in [0, T]\}$. Then $p, c, \mu \in C^2(Q_T)$. And (18)~(20) are satisfied in classical sense.

The global and explicit formulation of moving speed of boundary is convenient for the flow map formulation of $\Omega(t)$ (Proposition 2) in next section.

3 Analysis on the free boundary model and the well mixed limit

This section is devoted to analyzing the free boundary model (17)~(21). First we give basic properties which shed some light on the structure of solutions, then we study the asymptotic behavior of the density fraction μ . In a special case, we show that the density fraction μ converges to a spatial homogeneous state within the tumor region $\Omega(t)$ as t goes to infinity. Moreover, the convergence is exponential. We call this phenomenon the “well-mixed” limit.

3.1 Well-posedness, characteristic structure and boundness of μ

In this subsection, we give some basic properties for the free boundary model. In particular we prove the characteristic structure of the density fraction μ which is useful in analyzing its asymptotic behavior.

First, we have the following proposition on the moving speed of $\partial\Omega(t)$.

Proposition 1. *For $T > 0$, suppose (Ω, p, c, μ) is a solution of the free boundary system (17)~(21) which satisfies Assumption 1 and 2 on the time interval $(0, T)$. Then the moving speed of the boundary $\partial\Omega(t)$ in normal direction is positive, that is,*

$$V_n = -\nabla p \cdot \mathbf{n} > 0,$$

for every $x \in \partial\Omega(t)$ and $t \in (0, T)$.

Proof. From Assumption 1 we have $\Delta p = -(\mu G + (1 - \mu)(G - D)) \leq 0$ for all $x \in \Omega(t)$, thus p achieves its minimum in $\overline{\Omega(t)}$ at $\partial\Omega(t)$. Thanks to the Dirichlet zero boundary condition, every point on $\partial\Omega(t)$ is a minimum point. Thus by Hopf's lemma we have $\frac{\partial p}{\partial n} < 0$ for all $x \in \partial\Omega(t)$, unless $p(\cdot, t) \equiv 0$ in $\Omega(t)$. The latter case implies $\Delta p \equiv 0$ which contradicts the Assumption 1. \square

Proposition 1 ensures that we do not need a boundary condition for the density fraction μ . To give a clear statement of its useful characteristic structure, we first give a reformulation of $\Omega(t)$ through the following flow map:

$$\begin{cases} \frac{dx}{dt}(t, y) = -\nabla p(x(t, y), t), \\ x(0, y) = y \in \overline{\Omega(0)}. \end{cases} \quad (22)$$

Well-posedness of this flow map is stated in the following proposition.

Proposition 2. *For $T > 0$, suppose (Ω, p, c, μ) is a solution of the free boundary system (17)~(21) which satisfies Assumption 1 and 2 on the time interval $(0, T)$. Then the followings are true.*

1. *The solution of the flow map (22) $x(t, y)$ exists and is unique for all initial $y \in \overline{\Omega(0)}$, $t \in [0, T)$.*
2. *Set $X_{t,0}$ be the map defined on $\overline{\Omega(0)}$ such that $X_{t,0}(y) = x(t, y)$ for $t \geq 0$. Then $X_{t,0}$ is a homeomorphism from $\overline{\Omega(0)}$ to $\overline{\Omega(t)}$. In particular for all initial $x \in \overline{\Omega(t)}$ there exists a unique $y \in \overline{\Omega(0)}$ such that $x = X_{t,0}(y) = x(t, y)$.*

Note well-posedness of (22) for x at $\partial\Omega(t)$ is implied by Assumption 2. The proof of Proposition 2 is straightforward and we postpone it to Appendix A. With this flow map formulation of $\Omega(t)$, we could state the characteristics structure of μ . Consider the following characteristic ODE system for the quasi-linear equation (18):

$$\begin{cases} \frac{dx}{dt}(t, y) = -(\nabla p)(x(t, y), t), \\ \frac{dz}{dt}(t, y) = -zK_1 + (1 - z)K_2 + Dz(1 - z), \\ x(0, y) = y \in \overline{\Omega(0)}, \\ z(0, y) = \mu_0(y). \end{cases} \quad (23)$$

Here the transition rates K_1, K_2 in the second equation depend on the nutrient at point $x(t, y)$ and time t , i.e., $K_i = K_i(c(x(t, y), t))$, $i = 1, 2$. We use the shorthand notation to save space. In (23) z can be seen as the Lagrangian representation of the density fraction μ . This fact is stated in the following proposition.

Proposition 3. *For $T > 0$, suppose (Ω, p, c, μ) is a solution of the free boundary system (17)~(21) which satisfies Assumption 1 and 2 on the time interval $(0, T)$. Then for all $x \in \overline{\Omega(t)}$, $t \in (0, T)$ there exists a $y \in \overline{\Omega(0)}$ such that $x = x(t, y)$ and we have $\mu(x, t) = z(t, y)$. Here x, z are the characteristic ODE as in (23).*

Proof. Proposition 2 ensures that for all $x \in \Omega(t)$ there exists a unique $y \in \Omega(0)$ such that $x = x(t, y)$. Then the following computation is standard:

$$\begin{aligned} \frac{d}{ds}\mu(x(s, y), s) &= \frac{\partial \mu}{\partial t} - (\nabla \mu) \cdot (\nabla p) \\ &= -\mu K_1 + (1 - \mu)K_2 + D\mu(1 - \mu). \end{aligned}$$

Thus $\mu(x(\cdot, y), \cdot)$ shares the same ODE and the initial value with $z(\cdot, y)$ in (23), and one obtains $\mu(x, t) = z(t, y)$. \square

Proposition 3 is helpful in the proof of the uniform convergence of the “well-mixed” limit in next subsection. With this characteristic structure, now it is easy to give a point-wise bound for μ as follows.

Corollary 1. *For $T > 0$, suppose (Ω, p, c, μ) is a solution of the free boundary system (17)~(21) which satisfies Assumption 1 and 2 on the time interval $(0, T)$. And the parameters satisfy (3). Then the density fraction $\mu(x, t) \in [0, 1]$, for all $x \in \bar{\Omega}(t)$ and $t \in (0, T)$.*

Proof. Let us look at $z(t, y)$, the Lagrangian representation of μ in (23). By Proposition 3 it suffices to show that $z(t, y) \in [0, 1]$ for all $y \in \Omega(0)$ and $t \in (0, T)$. Recall the ODE for z (23):

$$\frac{dz}{dt} = -zK_1 + (1-z)K_2 + Dz(1-z).$$

Notice that initially $z(0, y) = \mu(y, 0) = \mu_0(y) \in [0, 1]$ by (17). Then the result follows from that $K_1, K_2 > 0$ in (3) and the comparison principle. \square

3.2 Asymptotic behavior for μ : the well-mixed limit

This subsection is devoted to analyzing the asymptotic behavior of density fraction μ as time t goes to infinity. For simplicity of analysis, we make the following assumption.

Assumption 3. *The transition rates K_1, K_2 are constants.*

With Assumption 3, we can show that the density fraction μ will converge to a spatial-homogeneous steady state $\mu \equiv \mu^*$, $x \in \Omega(t)$, where $\mu^* \in [0, 1]$ is a constant. And we characterize it from two aspects: a uniform convergence result (Theorem 1) and convergence in “ L^{2n} norm” ($n \in \mathbb{N}^+$) under a family of conditions (Theorem 2).

First we analyze the reaction term for μ . Let $f(\mu)$ denotes the right hand side in (18), we have

$$f(\mu) = -\mu K_1 + (1-\mu)K_2 + D\mu(1-\mu) = -D\mu^2 + (D - K_1 - K_2)\mu + K_2. \quad (24)$$

We observe that f is a quadratic function in μ . Recall in our model assumption (2) the extra death rate due to autophagy $D > 0$. And in (3) the transition rates $K_1, K_2 > 0$. Thus we observe that $f(0) = K_2 > 0$, $f(1) = -K_1 < 0$ and $-\frac{K_2}{D} < 0$. This implies that the two roots $\nu^* < \mu^*$ of f satisfies that $\nu^* < 0$, $\mu^* \in (0, 1)$. Precisely we have

$$\nu^* = \frac{D - K_1 - K_2 - \sqrt{E}}{2D}, \quad \mu^* = \frac{D - K_1 - K_2 + \sqrt{E}}{2D}, \quad (25)$$

where $E = D^2 + (K_1 + K_2)^2 - 2DK_1 + 2DK_2$.

With this information we could characterize the asymptotic behavior of the reaction ODE $\frac{dz}{dt} = f(z)$, which we write as the following lemma.

Lemma 1. *Suppose (2), (3) and Assumption 3 are satisfied. Let $f(\mu)$ be the rate function as in (24) and $\nu^* < \mu^*$ be two roots of f as in (25). Consider the following ODE,*

$$\begin{cases} \frac{dz}{dt}(t) = f(z(t)) = -D(z(t) - \nu^*)(z(t) - \mu^*), & t \geq 0. \\ z(0) = z_0. \end{cases}$$

If initial value $z_0 > \nu^$, then the solution $z(t)$ converges to μ^* exponentially as $t \rightarrow \infty$. Precisely, we have*

$$|z(t) - \mu^*| \leq \frac{\max\{z_0, \mu^*\} - \nu^*}{z_0 - \nu^*} e^{-D(\mu^* - \nu^*)t} |z_0 - \mu^*|. \quad (26)$$

Proof. From the comparison principle we know that if $z_0 \geq \mu^*$ then $z(t) \geq \mu^*$, for all $t \geq 0$, and thus $\frac{dz}{dt}(t) = -D(z(t) - \nu^*)(z(t) - \mu^*) \leq 0$, for all $t \geq 0$, which means the solution is decreasing. Similarly from the comparison principle if $z_0 \in (\nu^*, \mu^*)$ then the solution will stay in this interval and thus $\frac{dz}{dt}(t) = -D(z(t) - \nu^*)(z(t) - \mu^*) \geq 0$, which means the solution is increasing. In both cases one has

$$\nu^* < z(t) < \max\{z_0, \mu^*\}, \quad \forall t \geq 0.$$

On the other hand with elementary calculation we have

$$|z(t) - \mu^*| = \frac{|z(t) - \nu^*|}{|z_0 - \nu^*|} e^{-D(\mu^* - \nu^*)t} |z_0 - \mu^*|.$$

Then the result follows from $0 < z(t) - \nu^* \leq \max\{z_0, \mu^*\} - \nu^*$. \square

Applying Lemma 1 along the characteristics of density fraction μ (23), we obtain the following uniform convergence result:

Theorem 1. Suppose (Ω, p, c, μ) is a solution of the free boundary system (17)~(21) which satisfies Assumption 1 and 2 on the time interval $(0, \infty)$. Suppose (2), (3) and Assumption 3 are satisfied. Let f be the rate function as in (24) and $\nu^* < \mu^*$ be two roots of f as in (25).

Then we have $\mu(x, t) \rightarrow \mu^*$ uniformly for $x \in \overline{\Omega(t)}$ as $t \rightarrow \infty$. Here “uniformly” means $\|\mu(\cdot, t) - \mu^*\|_{C(\overline{\Omega(t)})} \rightarrow 0$ as $t \rightarrow \infty$. In addition, the convergence is exponentially fast in the sense that

$$\|\mu(\cdot, t) - \mu^*\|_{C(\overline{\Omega(t)})} \leq Ae^{-D(\mu^* - \nu^*)t} \|\mu(\cdot, 0) - \mu^*\|_{C(\overline{\Omega(0)})}, \quad (27)$$

where $A > 0$ is some constant.

Proof. By Proposition 3, for all x in $\overline{\Omega(t)}$, despite $\Omega(t)$ is expanding, we can always trace back along characteristics to find an initial position $y \in \overline{\Omega(0)}$ such that

$$\mu(x, t) = z(t, y), \quad x = x(t, y),$$

where $x(t, y)$ is the characteristics of μ and $z(t, y)$ is the Lagrangian representation for μ as in (23). Since with initial condition (17), $z(0, y) = \mu(y, 0) = \mu_0(y) \in [0, 1] \subset (\nu^*, +\infty)$, by Lemma 1 we have

$$\begin{aligned} |z(t, y) - \mu^*| &\leq \frac{\max\{z(0, y), \mu^*\} - \nu^*}{z(0, y) - \nu^*} e^{-D(\mu^* - \nu^*)t} |z(0, y) - \mu^*| \\ &\leq \max_{z_0 \in [0, 1]} \left\{ \frac{\max\{z_0, \mu^*\} - \nu^*}{z_0 - \nu^*} \right\} e^{-D(\mu^* - \nu^*)t} |z(0, y) - \mu^*|, \end{aligned}$$

for all $y \in \overline{\Omega(0)}$. With straightforward computation, one has

$$\frac{\max\{z_0, \mu^*\} - \nu^*}{z_0 - \nu^*} = \frac{\max\{z_0 - \nu^*, \mu^* - \nu^*\}}{z_0 - \nu^*} = \max\left\{1, \frac{\mu^* - \nu^*}{z_0 - \nu^*}\right\} \leq \frac{\mu^* - \nu^*}{-\nu^*},$$

when $z_0 \in [0, 1]$. Then we conclude

$$|z(t, y) - \mu^*| \leq \frac{\mu^* - \nu^*}{-\nu^*} e^{-D(\mu^* - \nu^*)t} |z(0, y) - \mu^*|.$$

Taking maximum for $y \in \overline{\Omega(0)}$ at both sides, we complete the proof. And the coefficient $A > 0$ in (27) can be taken as $\frac{\mu^* - \nu^*}{-\nu^*}$. \square

Note that the convergence can also be observed directly through the equation of μ (18), which is equivalent to

$$\partial_t \left(\ln \frac{|\mu - \mu^*|}{|\mu - \nu^*|} \right) - \nabla p \cdot (\nabla \ln \frac{|\mu - \mu^*|}{|\mu - \nu^*|}) = -D(\mu^* - \nu^*).$$

The uniform convergence result is illustrated in Figure 2, where we numerically simulate the compressible model with large γ . We plot the densities of total cells n and autophagic cells $n_2 = (1 - \mu)n$. We also plot the theoretical value for the density of autophagic cells in the “well-mixed” limit $(1 - \mu^*)n$ for comparison. Initially the value of μ is highly spatially heterogeneous, and as time evolves, the tumor expands while the two types of cells mix towards the equilibrium ratio μ^* . In particular when $t = 3$ autophagic cells and normal cells are effectively “well-mixed”.

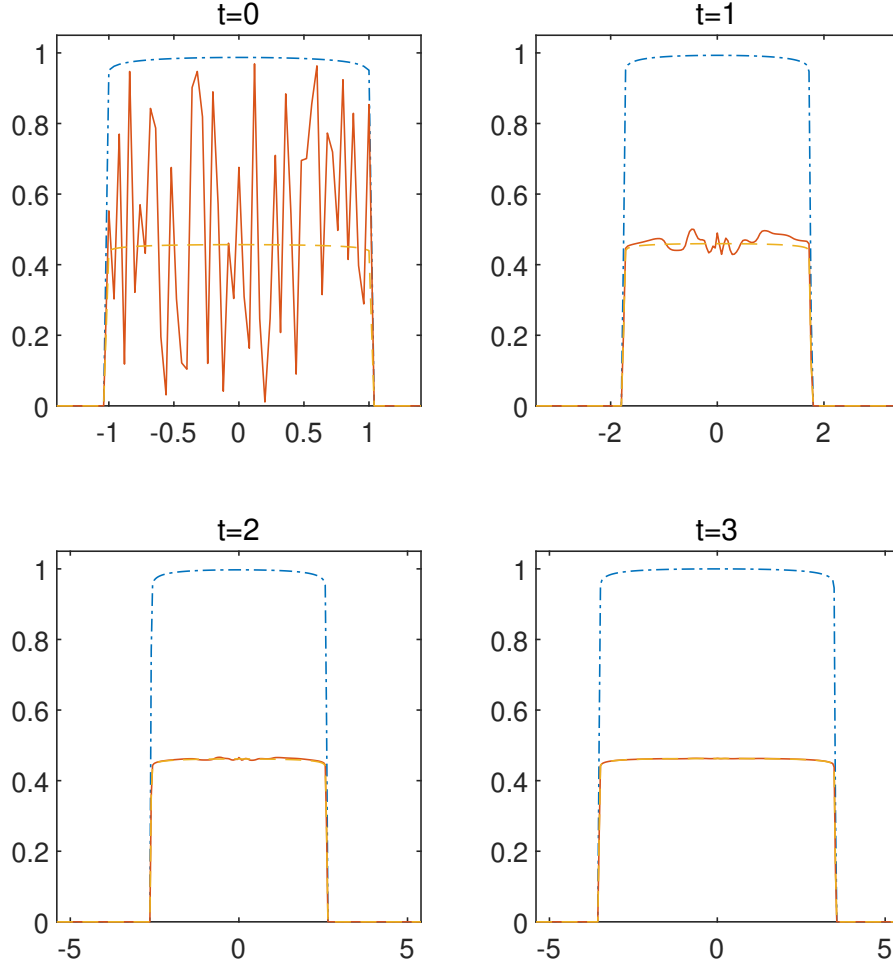


Figure 2: Densities of cells at time $t = 0, 1, 2, 3$ with a heterogeneous initial density fraction. Blue dash-dotted line: the total density n . Red solid line: the density of autophagic cells n_2 . Orange dashed line: theoretical value for density of autophagic cells in the “well-mixed” limit. Parameters: $\gamma = 80$, $G(c) = gc$, $\psi(c) = c$, $K_1 = K_2 = 1$, $g = 1$, $a = 0.4$, $D = 0.3$.

Besides this uniform convergence result, we consider the “ L^q estimate” on $\|\mu - \mu^*\|_{L^q(\Omega(t))}$ ($1 \leq q < +\infty$). If the domain is fixed, then the decay of $|\mu - \mu^*|$ in L^q norm is trivial since the L^∞ norm can control the L^q norm. The difference is here we are facing an expanding domain. We first give an intuitive analysis. From Theorem 1 the “pointwise” convergence of $|\mu - \mu^*|$ is exponential with the rate $r_1 := D(\mu^* - \nu^*)$. Thus, intuitively one has

$$\int_{\Omega(t)} |\mu - \mu^*|^q dx \approx C|\Omega(t)| \exp\{-qr_1 t\}. \quad (28)$$

As we will see in the next section (see discussion about (41),(44)), when the nutrient provided by autophagy is relatively sufficient, $|\Omega(t)|$ may also grow exponentially, i.e.,

$$|\Omega(t)| \approx |\Omega(0)| \exp\{r_2 t\}, \quad (29)$$

for some $r_2 > 0$. Combine (29) with (28), formally we have

$$\int_{\Omega(t)} (\mu - \mu^*)^q dx \approx C|\Omega(0)| \exp\{(r_2 - qr_1)t\}. \quad (30)$$

Thus we are facing a competition of exponential growth and exponential decay. Intuitively the L^q norm ($q \geq 1$) $\|\mu - \mu^*\|_{L^q(\Omega(t))}$ will exponentially decay if and only if $q > \frac{r_2}{r_1}$. In the following, we do not investigate (30) in details but give a family of sufficient conditions for the decay in “ L^{2n} norm” ($n \in \mathbb{N}^+$) to be held. For preparation, first we give an a priori estimate on the concentration of nutrients c .

Lemma 2. For $T > 0$, suppose (Ω, p, c, μ) is a solution of the free boundary system (17)~(21) which satisfies Assumption 1 and 2 on the time interval $(0, T)$, $T > 0$. And suppose (2)~(4) are true. Then we have

$$c(x, t) \leq \max\{c_B, c_0\},$$

for all $x \in \overline{\Omega(t)}$, $t \in (0, T)$. Recall c_B is the boundary value of c and c_0 is the threshold concentration such that $\psi(c_0) = a$ as in (4).

The proof is straightforward from the maximum principle.

Proof. For $t \in (0, T)$, suppose $c(\cdot, t)$ reaches its maximum in $\overline{\Omega(t)}$ at $x^* \in \overline{\Omega(t)}$. It suffices to prove $c^* := c(x^*, t) \leq \max\{c_0, c_B\}$. If $x^* \in \partial\Omega(t)$, then $c^* = c_B$. It is done.

Otherwise the maximum point x^* lies in $\Omega(t)$, and one obtains $\Delta c(x^*, t) \leq 0$. Thus from the equation (20) for c , one gets

$$\psi(c^*) \leq (1 - \mu)a \leq a = \psi(c_0). \quad (31)$$

The second inequality uses that $\mu(x, t) \in [0, 1]$ by Corollary 1. And the last equality is the definition of c_0 (4). Thus we obtain $c^* \leq c_0$ since $\psi'(c) > 0$ as in (4). \square

Thanks to Lemma 2, we could control the concentration of nutrients c . Now we give a family of sufficient conditions for $\|\mu - \mu^*\|_{L^{2n}(\Omega(t))}$ ($n \in \mathbb{N}^+$) to exponentially decay:

Theorem 2. Suppose (Ω, p, c, μ) is a solution of the free boundary system (17)~(21) which satisfies Assumption 1 and 2 on the time interval $(0, \infty)$. And suppose (2)~(4) and Assumption 3 are true. Let f be the rate function as in (24) and $\nu^* < \mu^*$ be two roots of f as in (25). Then for $n \in \mathbb{N}^+$, $\|\mu(\cdot, t) - \mu^*\|_{L^{2n}(\Omega(t))}$ will exponentially decay if

$$G(\max\{c_B, c_0\}) - D < 2nK_2. \quad (32)$$

Precisely, we have

$$\|\mu(\cdot, t) - \mu^*\|_{L^{2n}(\Omega(t))} \leq \exp\{-Ct\} \|\mu(\cdot, 0) - \mu^*\|_{L^{2n}(\Omega(0))},$$

where

$$C = \frac{-\nu^*}{1 - \nu^*} K_1 + \frac{1}{2n} (2nK_2 - G(\max\{c_0, c_B\}) + D) > 0.$$

Proof. Let $\phi(\mu) = (\mu - \mu^*)^{2n}$, then by Reynolds's transport theorem,

$$\frac{d}{dt} \int_{\Omega(t)} \phi(\mu) dx = \int_{\Omega(t)} \phi'(\mu) \mu_t dx + \int_{\partial\Omega(t)} \phi(\mu) \left(-\frac{\partial p}{\partial n}\right) dS.$$

Since by the divergence theorem

$$\int_{\partial\Omega(t)} \phi(\mu) \left(-\frac{\partial p}{\partial n}\right) dS = \int_{\Omega(t)} -\phi'(\mu) \nabla \mu \cdot \nabla p - \phi(\mu) \Delta p dx,$$

we have

$$\begin{aligned} \frac{d}{dt} \int_{\Omega(t)} \phi(\mu) dx &= \int_{\Omega(t)} \phi'(\mu) (\mu_t - \nabla \mu \cdot \nabla p) dx + \int_{\Omega(t)} \phi(\mu) (-\Delta p) dx \\ &= \int_{\Omega(t)} (\phi'(\mu) f(\mu) - \phi(\mu) \Delta p) dx, \end{aligned} \quad (33)$$

where f is as in (24). Notice that

$$\phi'(\mu) f(\mu) = -2nD(\mu - \mu^*)^{2n}(\mu - \nu^*) = -2nD\phi(\mu)(\mu - \nu^*).$$

Plugging it in (33) and substituting the equation for p (19) one obtains

$$\begin{aligned} \frac{d}{dt} \int_{\Omega(t)} \phi(\mu) dx &= \int_{\Omega(t)} \phi'(\mu) f(\mu) - \phi(\mu) \Delta p dx \\ &= \int_{\Omega(t)} -\phi(\mu) (2nD(\mu - \nu^*) - G(c)\mu - (G(c) - D)(1 - \mu)) dx \\ &= - \int_{\Omega(t)} \phi(\mu) (2nD(\mu - \nu^*) - D\mu - (G(c) - D)) dx, \end{aligned} \quad (34)$$

By Lemma 2 we have $c(x, t) \leq \max\{c_0, c_B\}$, thus $G(c) - D \leq G(\max\{c_0, c_B\}) - D =: G_2^*$. Applying this inequality to (34), we have

$$\frac{d}{dt} \int_{\Omega(t)} \phi(\mu) dx \leq - \int_{\Omega(t)} \phi(\mu) (2nD(\mu - \nu^*) - D\mu - G_2^*) dx \quad (35)$$

Thanks to Gronwall's inequality, it suffices to show that

$$\Phi(\mu) \triangleq 2nD(\mu - \nu^*) - D\mu - G_2^*$$

has a positive lower bound.

Note that $\Phi(\mu)$ is a linear function of $\mu \in [0, 1]$ with slope $\Phi'(\mu) = (2n - 1)D > 0$. Thus it is equivalent to show that

$$\Phi(0) = -G_2^* - 2nD\nu^* > 0.$$

Recall that ν^* is a negative root of f :

$$D\nu^*(1 - \nu^*) - K_1\nu^* + K_2(1 - \nu^*) = 0.$$

Thus, multiply $\Phi(0)$ by $(1 - \nu^*) > 0$, we conclude that

$$\begin{aligned} \Phi(0)(1 - \nu^*) &= -2nK_1\nu^* + 2nK_2(1 - \nu^*) - (1 - \nu^*)G_2^* \\ &= (1 - \nu^*)(2nK_2 - G_2^*) - 2nK_1\nu^* > 0. \end{aligned}$$

Then we obtain a positive lower bound for Φ

$$\Phi(\mu) \geq \Phi(0) \geq (2nK_2 - G_2^*) + \frac{-\nu^*}{1 - \nu^*} 2nK_1 > 0, \quad \forall \mu \in [0, 1].$$

Apply this to (35), we obtain

$$\frac{d}{dt} \int_{\Omega(t)} \phi(\mu) dx \leq -C \int_{\Omega(t)} \phi(\mu) dx,$$

where $C = (2nK_2 - G_2^*) + \frac{-\nu^*}{1 - \nu^*} 2nK_1$. Then by Gronwall's inequality the proof is completed. \square

In Figure 3 we numerically simulate the compressible model to illustrate the competition between exponential growth of $|\Omega(t)|$ and exponential decay of $|\mu - \mu^*|$. We plot the evolution of $\|\mu(\cdot, t) - \mu^*\|_{L^{2n}(\overline{\Omega(t)})}$ with different n under two parameters regimes. In the first regime (Figure 3a) K_2 is large and the L^2, L^4, L^8 norm decay fast. In the second regime (Figure 3b) K_2 is small. L^2 norm tends to diverge to infinity but L^4, L^8 norm are decreasing. This also indicates that the condition (32) in Theorem 2 may not be sharp since it is violated for all the three cases L^2, L^4, L^8 in the second regime.

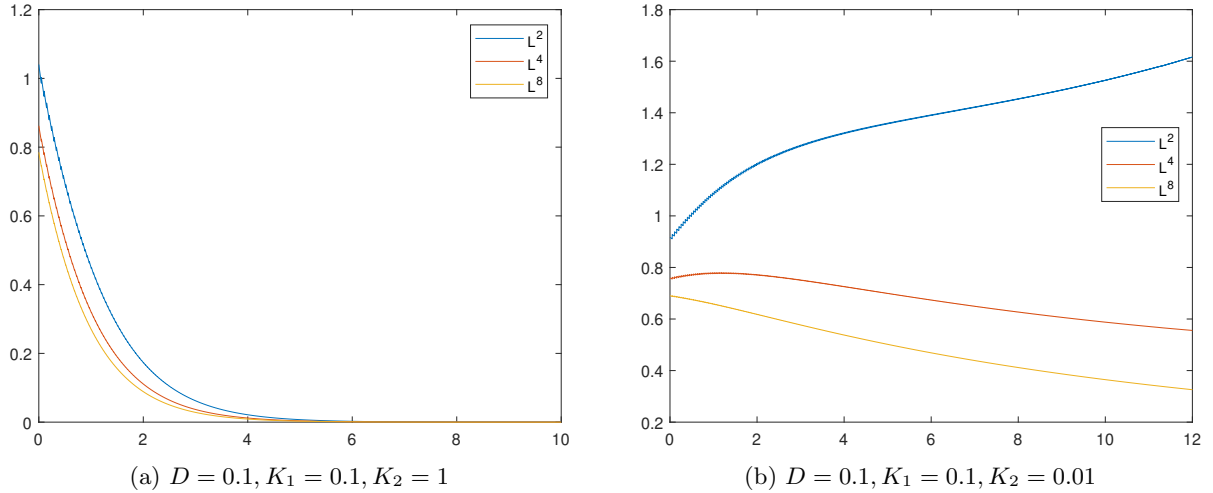


Figure 3: Evolution of $\|\mu(\cdot, t) - \mu^*\|_{L^{2n}(\overline{\Omega(t)})}$ with respect to time under different parameter regimes. Parameters: $\gamma = 80$, $G(c) = gc$, $\psi(c) = c$ with $g = 1, a = 0.5$ and $c_B = 1$. Here the threshold value of nutrient concentration $c_0 = 0.5$.

The “well-mixed” limit shows that under Assumption 1, the density fraction $\mu(x, t)$ will converge to a spatial-homogeneous constant state exponentially fast. This allows us to further simplify the model by taking μ to be a constant for all $x \in \overline{\Omega(t)}$, i.e. $\mu \equiv \mu^*$, where μ^* is the root in $(0, 1)$ of f in (24). For this simplified model with constant μ , it is convenient to draw analytical solutions as in [24] and to further study the behavior of the free boundary model, as we do in the next section.

4 Analytical and numerical study on Cauchy problem

In this section, we first derive an analytical solution for the free boundary model with constant μ in one-dimensional symmetric case. The analytical solution shows that when the nutrient supply rate by autophagic cells a is relatively larger than the extra death rate D from self-killing, such a mechanism will result in exponential growth rate of the tumor, in contrast to the linear growth rate in a related tumor-nutrient model in [24]. The essential reason is that in the presence of the autophagy, sufficient nutrients are available to the tumor, whatever big it is.

Also, we do numerical simulations on the compressible model with large γ for demonstration.

4.1 An one-dimensional analytic solution with constant μ

The “well-mixed” limit in Section 3 shows that under Assumption 3, the density fraction μ has a constant steady state: $\mu \equiv \mu^*$, for all $x \in \Omega(t)$. Here μ^* as in (25) is the root of f (24). This allows use to simplify the model by set μ to be the constant μ^* , i.e., $\mu \equiv \mu^*$, $\forall x \in \Omega(t), t \geq 0$. Then the model (17)~(21) reduces to the evolution of (Ω, p, c) (19)~(21):

$$\begin{cases} -\Delta p = \mu G(c) + (1 - \mu)(G(c) - D), & x \in \Omega(t). \\ p = 0, & x \in \partial\Omega(t). \\ -\Delta c + \psi(c) = (1 - \mu)a, & x \in \Omega(t), \\ c = c_B > 0, & x \in \partial\Omega(t), \\ V_n = -\nabla p \cdot \mathbf{n}, & x \in \partial\Omega(t). \end{cases} \quad (36)$$

To derive an analytical solution, we shall specify the parameters. For the net growth rate of normal cells G we assume the proliferation rate is proportional to the concentration of nutrients c with a factor g and we omit the death rate of normal cells for simplicity. Thus $G(c) = gc$. For the consumption rate $\psi(c)$, we assume it is proportional to c . Precisely we choose $\psi(c) = c$. And since nutrient is relatively sufficient at the boundary of tumor, we assume the threshold value for autophagy cells c_0 in (4) is less than the boundary value for the concentration of nutrients c_B . Note when $\psi(c) = c$, $c_0 = a$. To summarize, we assume

$$G(c) = gc, \quad \psi(c) = c, \quad a < c_B. \quad (37)$$

Furthermore, for simplicity we consider one-dimensional symmetric case, when the tumor region $\Omega(t) = (-R(t), R(t))$. With these choices of parameters, (36) becomes

$$\begin{cases} -\frac{d^2}{dx^2} p = gc - (1 - \mu)D, & x \in (-R(t), R(t)), \\ p = 0, & x = \pm R(t). \\ -\frac{d^2}{dx^2} c + c = (1 - \mu)a, & x \in (-R(t), R(t)), \\ c = c_B > 0, & x = \pm R(t). \\ \frac{dR}{dt} = -\frac{dp}{dx} \Big|_{x=R(t)}. \end{cases} \quad (38)$$

System (38) is essentially a single-species model. And the following derivation of an analytical solution is similar to that in [24].

First we solve c from the equation of nutrients. With the boundary condition $c(R(t)) = c_B$ and the symmetric condition $\frac{d}{dx}c|_{x=0} = 0$, we obtain the expression of c :

$$\begin{aligned} c(x, t) &= (1 - \mu)a + \frac{c_B - (1 - \mu)a}{\cosh(R(t))} \cosh(x) \\ &= \frac{c_B}{\cosh(R(t))} \cosh(x) + (1 - \mu)a \left(1 - \frac{\cosh(x)}{\cosh(R(t))}\right). \end{aligned} \quad (39)$$

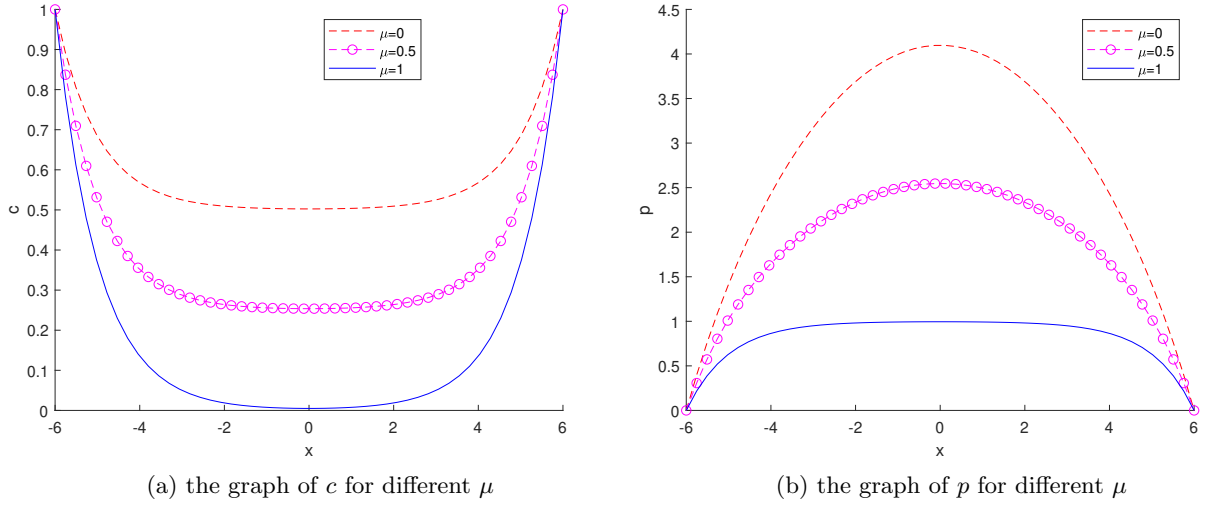


Figure 4: The graph of the concentration of nutrients c and pressure p for different μ . When $\mu = 1$ there is no autophagic cells, when $\mu = 0$ all cells are autophagic cells. Parameters: $c_B = 1, a = 0.5, g = 1, D = 0.3$.

Plugging (39) into the equation for p , one gets

$$-\frac{d^2}{dx^2}p = gc - (1 - \mu)D = \frac{g(c_B - (1 - \mu)a)}{\cosh(R(t))} \cosh(x) + (1 - \mu)ga - (1 - \mu)D.$$

Together with boundary condition $p(\pm R(t)) = 0$, the solution of p is

$$p(x, t) = -\frac{g(c_B - (1 - \mu)a)}{\cosh(R(t))} \cosh(x) - \frac{1}{2}(1 - \mu)(ga - D)x^2 + C, \quad (40)$$

where the coefficient of linear term x is 0 by symmetry and C could be determined from $p(R(t)) = 0$. Actually $C = g(c_B - (1 - \mu)a) + \frac{1}{2}(1 - \mu)(ga - D)R(t)^2$.

In Figure 4 we plot the graph of pressure p and nutrients c with different μ . When all cells are normal cells ($\mu = 1$), in the middle of tumor the concentration of nutrients c decays to zero, and the profile of pressure p is flat, which indicates that the proliferation is limited. While in the presence of autophagic cells ($\mu = 0.5, 1$), the concentration of nutrients can maintain a basal level to support proliferation in the core of tumor, which leads to the bulge profile of p .

From (40) the moving speed of the boundary reads:

$$\frac{dR(t)}{dt} = -\frac{dp}{dx}|_{x=R(t)} = g(c_B - (1 - \mu)a) \tanh(R(t)) + (1 - \mu)(ga - D)R(t). \quad (41)$$

Whereas, when there is no autophagic cells (i.e., $\mu = 1$), the moving speed is, as that in [24]:

$$\frac{dR(t)}{dt} = gc_B \tanh(R(t)). \quad (42)$$

An essential difference brought by autophagy is the linear term on the right hand side of (41), compared to (42). Recall our choice of parameters (37), a bifurcation depending on the growth factor g , the nutrient supply rate by autophagy a and the extra death rate due to autophagy D arises:

1. When $ga > D$, the linear term will result in exponential growth, while when there is no autophagy the growth rate in (42) is nearly a constant, as plotted in Figure 5, which results in linear growth. Biologically this means when the nutrients supplied by autophagic cells are sufficient to offset its extra death, autophagy will significantly accelerate tumor growth.
2. While, on the contrary when $ga < D$, the solution may violate the non-negative Assumption 1 if $R(t)$ is large. This indicates when the extra death of autophagy D is dominant, autophagy may accelerate cells death and lead to formation of necrotic core.

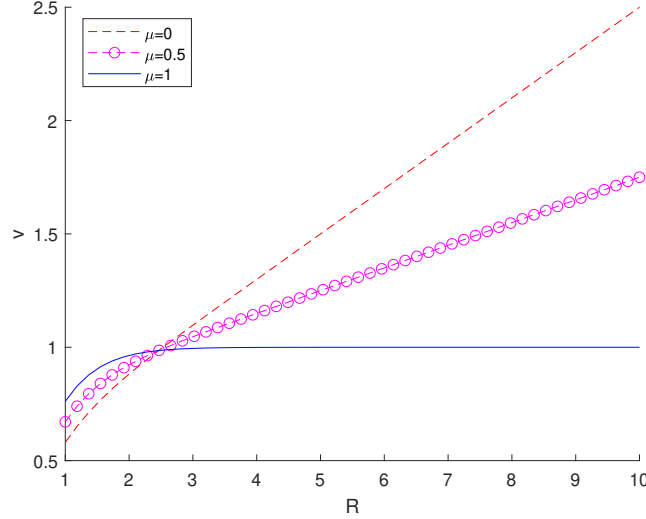


Figure 5: The moving speed of the boundary $v := \frac{dR(t)}{dt}$ w.r.t different R for different μ . When $\mu = 1$ there are only normal cells, and the growth rate tends to be constant which leads to a linear growth of R . In the presence of autophagy, the growth rate tends to be linear in R , which leads to an exponential growth of R . Parameters: $c_B = 1, a = 0.5, g = 1, D = 0.3$.

We could understand the exponential growth in the presence of autophagy in a more direct way. From the conversation of density, we have

$$\frac{dR(t)}{dt} = \frac{1}{2} \int_{-R(t)}^{R(t)} (G(c) - (1 - \mu)D) dx. \quad (43)$$

By the maximum principle we have a lower bound for c , precisely $c \geq \min\{c_B, (1 - \mu)a\} = (1 - \mu)a$. Thus we have $G(c) \geq (1 - \mu)ga$. Combine this with (43), we obtain

$$\frac{dR(t)}{dt} = \frac{1}{2} \int_{-R(t)}^{R(t)} (G(c) - (1 - \mu)D) dx \geq \frac{1}{2} \int_{-R(t)}^{R(t)} (1 - \mu)(ga - D) dx = (1 - \mu)(ga - D)R(t).$$

Thus we get the exponential growth of R :

$$R(t) \geq \exp\{(1 - \mu)(ga - D)t\}R(0). \quad (44)$$

This reasoning can easily extend to higher dimensional cases with similar assumptions.

4.2 Numerical simulation for the Cauchy problem

In this subsection, we numerically simulate the compressible PDE model (5) in one-dimensional with large γ to demonstrate the incompressible limit and analysis on the moving speed of the boundary.

For the numerical scheme, we adapt the prediction-correction framework in [23] which we present in details in Appendix B. Our computations are in one-dimension. We choose the spatial step $\Delta x = 0.04$ and the temporal step $\Delta t = 0.002$.

We recall in the compressible model, densities of normal cells n_1 and autophagic cells n_2 satisfy the following system:

$$\begin{cases} \frac{\partial n_1}{\partial t} - \nabla \cdot (n_1 \nabla p) = G(c)n_1 - K_1 n_1 + K_2 n_2, \\ \frac{\partial n_2}{\partial t} - \nabla \cdot (n_2 \nabla p) = (G(c) - D)n_2 + K_1 n_1 - K_2 n_2, \\ p = \frac{\gamma}{\gamma - 1} (n_1 + n_2)^{\gamma - 1}, \end{cases}$$

We choose compactly supported total density $n = n_1 + n_2$ for initial data. Thus $\Omega(t) := \{x : n(x, t) > 0\}$ is a bounded domain for all $t > 0$, which allows us to choose the quasi-static case of (8) for the evolution of nutrients:

$$\begin{cases} -\Delta c + \psi(c)(n_1 + n_2) = an_2, & x \in \Omega(t), \\ c = c_B, & x \notin \partial\Omega(t). \end{cases}$$

And parameters are chosen of forms in (37).

First, to demonstrate the incompressible limit, we compare numerical solutions of total density n and pressure p for different γ with analytical solutions of the free boundary model ($\gamma = \infty$ formally). Initially we take $\Omega(0) = (-R, R)$

with $R = 1$ and specify the pressure p according to the analytical solution of free boundary model (40). Then the initial total density n is recovered from (6). We choose initial density fraction μ to be at the well-mixed constant μ^* , thus we could get initial density of two kinds of cells $n_1 = \mu^* n$ and $n_2 = (1 - \mu^*)n$. For different γ we numerically evolves this system till time $t = 1$. We plot these numerical solutions as well as the analytical solution. For total density n the analytical solution is $\mathbb{I}_{(-R(t), R(t))}$ while for pressure p that is given in (40). Here $R(t)$ is obtained by numerically solve the ODE (41). Results in Figure 6 show that as γ increases the numerical solutions get closer to the analytical solution of the free boundary model.

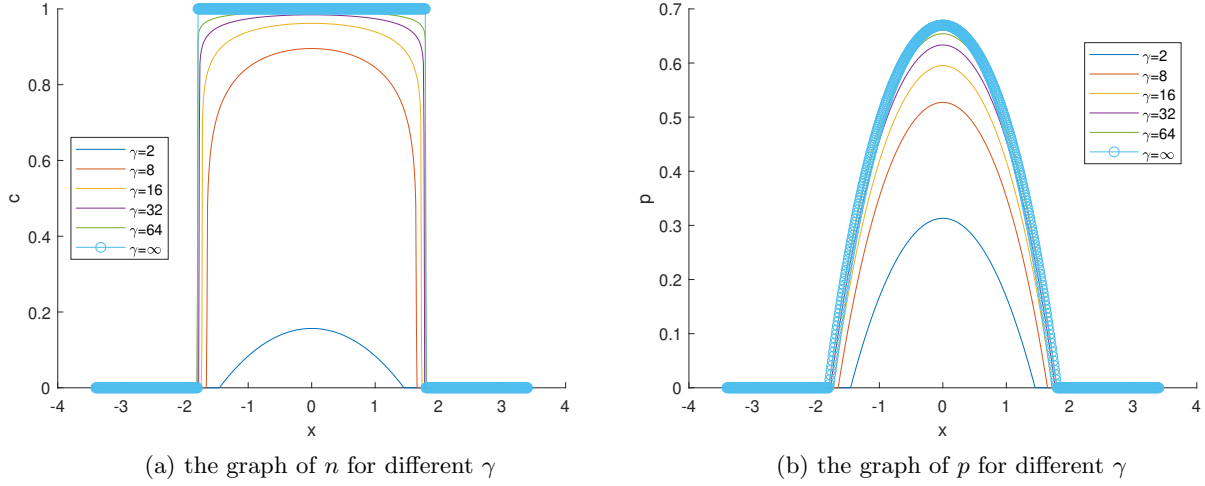


Figure 6: The graphs of the total density n and the pressure p for different γ at $t = 1$. $\gamma = \infty$ stands for the analytical solution of the free boundary problem. As γ increases, the solution of the compressible model approximates the solution of the free boundary model. Parameters: $g = 1, a = 0.5, D = 0.3, c_B = 1, K_1 = K_2 = 1$

Next, we investigate the boundary propagation speed, which are to be compared with the analytical results. For compressible models with large γ , we plot the evolution of radius with respect to time in two cases: $ga = D$ and $ga > D$ in Figure 7a. Results are close to the evolution of $R(t)$ in the free boundary model, i.e., the ODE (41). We also plot $\log R$ with respect to time in the case $ga > D$ to verify the exponential growth in Figure 7b. Numerical solutions are consistent with the analytical results: when $ga = D$ the growth is nearly linear and when $ga > D$ the radius tends to grow exponentially.

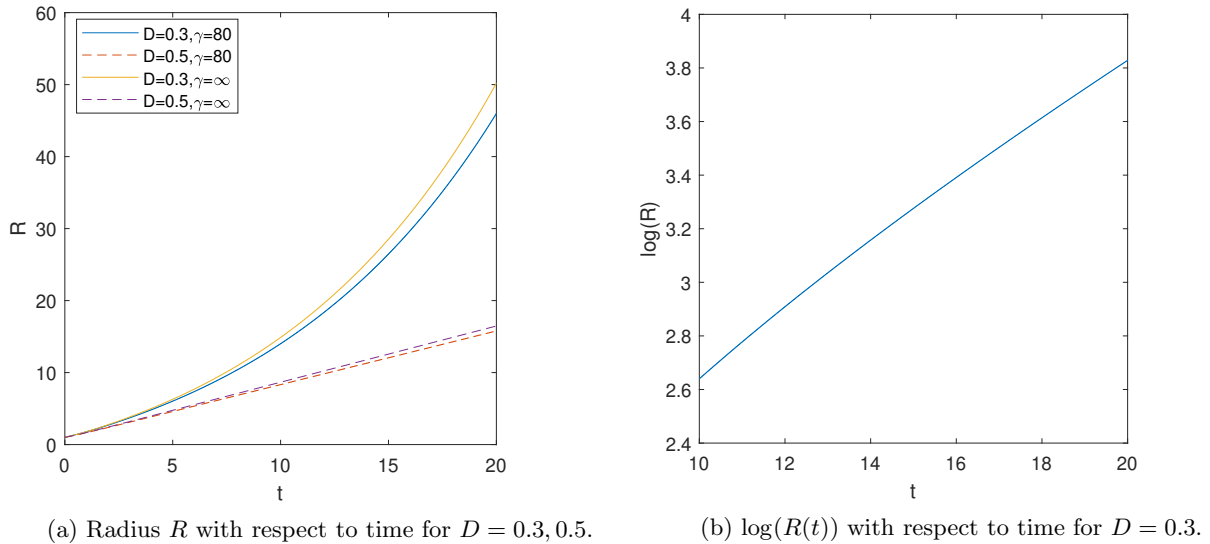


Figure 7: Growth of radius with different D . Other parameters $g = 1, a = 0.5$. Left: radius w.r.t. time. Solid line: $D = 0.3$ and thus $ga > D$. Dashed line: $D = 0.5$ and thus $ga = D$. Right: $\log R$ w.r.t. time for $D = 0.3$ for $t = 10$ to $t = 20$.

5 Numerical simulations with Neumann boundary condition

In this section we consider a cell density model for tumor growing in a bounded domain $\Omega \subset \mathbb{R}^n$, which can be seen as a modified version of the PDE system (5) with the Neumann boundary condition. We perform numerical simulations to study this model with more complicated settings than those in Section 3 and 4. Here we allow the transition rates K_1, K_2 to depend on the nutrient concentration, the formation of necrotic core and the dynamical boundary condition for the nutrient concentration c .

5.1 Setting of the Neumann problem

We extend the cell density model (5) to consider a tumor living in a bounded domain $\Omega \subset \mathbb{R}^n$. Since there shall be no flux of density going into or out of the domain, we have

$$n_i \frac{\partial p}{\partial \mathbf{n}} = 0, \quad x \in \partial\Omega, \quad t > 0, \quad i = 1, 2,$$

where \mathbf{n} is the outer normal vector of $\partial\Omega$. For motion of nutrients we consider (20) with $\varepsilon = 1$ and a Neumann boundary condition denotes the input nutrient flux from the boundary. Precisely, we consider the following system:

$$\begin{cases} \frac{\partial n_1}{\partial t} - \nabla \cdot (n_1 \nabla p) = G(c)n_1 - K_1(c)n_1 + K_2(c)n_2, & x \in \Omega, t > 0. \\ \frac{\partial n_2}{\partial t} - \nabla \cdot (n_2 \nabla p) = (G(c) - D)n_2 + K_1(c)n_1 - K_2(c)n_2, & x \in \Omega, t > 0. \\ n_i \frac{\partial p}{\partial \mathbf{n}} = 0, & x \in \partial\Omega, \quad i = 1, 2. \\ p = \frac{\gamma}{\gamma-1} (n_1 + n_2)^\gamma, \quad \gamma > 1. \\ \frac{\partial c}{\partial t} - \Delta c + \psi(c)(n_1 + n_2) = a n_2, & x \in \Omega, t > 0. \\ \frac{\partial c}{\partial \mathbf{n}} = -\lambda(t), & x \in \partial\Omega, \quad t > 0, \end{cases} \quad (45)$$

Here $\lambda(t) \geq 0$ denotes the input of nutrients from the boundary. System (45) is completed with non-negative initial values for n_1, n_2, c . We remark that porous media type tumor growth models for two species with Neumann boundary condition, without nutrients, has been considered in literature (e.g., [1, 2, 38]).

As before the parameters satisfy (2)~(4). In this section we allow $K_1(c), K_2(c)$ to vary with the concentration of nutrients in contrast to Assumption 3. Spatial heterogeneity in both total density n and the density fraction μ arises from heterogeneous nutrients availability. Also, in the middle of the tumor a necrotic core may form due to the lack of nutrients. For example, see Figure 8 where we plot the density of total cells n and autophagic cells n_2 in one dimensional with $\gamma = 2$ and $\gamma = 40$.

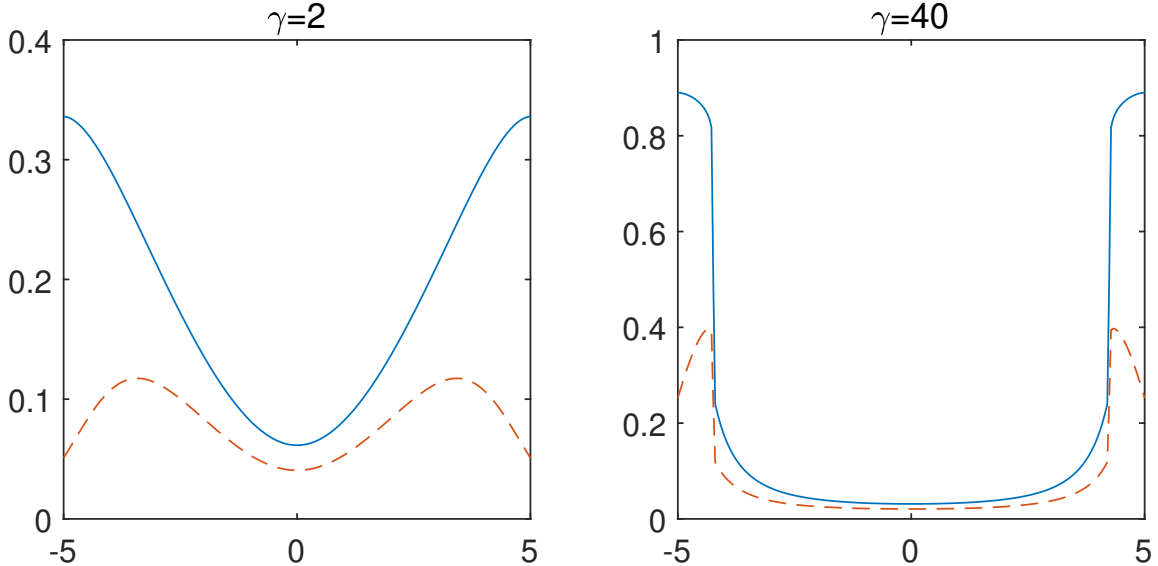


Figure 8: Densities of all cells n and of autophagic cells n_2 for $\gamma = 2, 40$ at $T = 20$. Solid line: the total density n . Dashed line: the density of autophagic cells n_2 . Plot at $T = 20$. Parameters: $G(c) = c - \delta$ with $\delta = 0.1$. $\psi(c) = c$. $D = 0.5, a = 0.5$. Transition rates satisfies $K_1(c) = k_{1,\max} \frac{\omega^4}{\omega^4 + c^4}$, $K_2(c) = k_{2,\max} \frac{c^4}{\omega^4 + c^4}$ as in (47), with $k_{1,\max} = k_{2,\max} = 3, \omega = 0.5$.

5.2 Numerical simulation

5.2.1 Parameters for numerical simulation

We carry out numerical simulation in a one-dimensional symmetric domain $\Omega = [-5, 5]$. We adapt the numerical scheme in [23] to treat the Neumann problem, with spatial grid length $\Delta x = 0.04$ and time step $\Delta t = 0.002$. The description of the numerical scheme is in Appendix B.

For the net growth rate $G(c)$ and the nutrient consumption rate $\psi(c)$ we choose the following forms unless otherwise specified:

$$G(c) = c - \delta, \quad \psi(c) = c, \quad (46)$$

where $\delta > 0$ is the death rate of normal cells.

For transition rates $K_1(c), K_2(c)$, we consider the following hull functions as in [18]:

$$\begin{aligned} K_1(c) &= k_{1,\max} \frac{\omega^4}{\omega^4 + c^4}, \\ K_2(c) &= k_{2,\max} \frac{c^4}{\omega^4 + c^4}. \end{aligned} \quad (47)$$

Here $k_{1,\max}, k_{2,\max} > 0$ can be used to adjust the magnitude of K_1, K_2 . And $\omega > 0$ reflects the scale of the concentration of nutrients c . Note that (47) satisfies $K_1'(c) < 0, K_2'(c) > 0$.

For the relation between n and p , we choose $\gamma = 40$.

Initially we let all cells be normal cells, i.e., the density fraction $\mu = 1$. And set the pressure p to be

$$p(x, 0) = \begin{cases} 1 - \frac{\cosh x}{\cosh R}, & |x| < R, \\ 0, & |x| \geq R, \end{cases}$$

which is a special case of (40) when $\mu = 1$. We choose $R = 4$ and recover the total density n from (6). For nutrients initially we set

$$c(x, 0) \equiv 1, \quad \forall x \in \Omega, \quad (48)$$

which is relatively sufficient.

5.2.2 Autophagy helps survivability

It is known that autophagy promotes cells survival under nutrient depletion. Experiments on yeasts have shown that cells with defective autophagy dramatically reduce their survivability under starvation while wild type cells maintain survival under the same condition [42], whose experiment data has been fitted by the ODE model [18]. This phenomenon is also observed in tumor growth [27].

In this model, $k_{1,\max}$ in (47) can be interpreted as the ability of autophagy. Since $K_1(c)$ is proportional to $k_{1,\max}$, when $k_{1,\max}$ is bigger, normal cells will change into autophagy cells with a faster rate. This results in a larger ratio of autophagic cells, at least heuristically, or in the simple case when the extra death rate $D = 0$.

Our goal in this subsection is to study the effects of autophagy under nutrient depletion by numerically simulating the Neumann problem (45) with different $k_{1,\max}$ under two kinds of nutrient input $\lambda(t)$.

First we consider the case when the nutrient input is constant in time, i.e., $\lambda(t) \equiv \lambda_0$. While initially the nutrient is sufficient (48), the nutrient input $\lambda(t)$ we choose is relatively small such that it is insufficient in the long term. From the evolution of total population $\int_{\Omega} n(x, t) dx$ in time (Figure 9 Left) one can see in a small initial period when the nutrient is sufficient, different $k_{1,\max}$ show little influence, while when the nutrient is no longer sufficient as time evolves, cells with higher $k_{1,\max}$ maintains a higher population, which is consistent with the ODE model in [18]. Spatially in the graph of total density n at a fixed time (Figure 9 Right), cells with higher $k_{1,\max}$ have a larger density as well as a smaller radius of necrotic core.

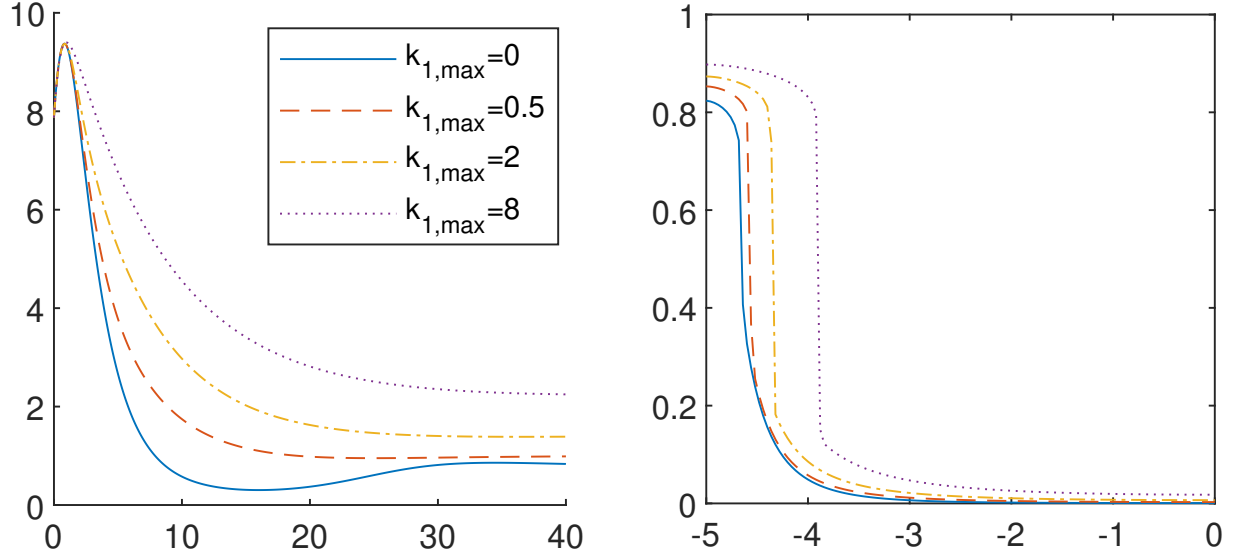


Figure 9: Left: Evolution of the total population $\int_{\Omega} n(x)dx$. Right: Plots of total density n with different $k_{1,\max}$. We only show the total density n in a half of the domain thanks to symmetry. Parameters: $\gamma = 40$. $a = 0.5$, $D = 0.1$, $\delta = 0.5$, $k_{2,\max} = 1$, $\omega = 0.5$. Nutrient input: $\lambda(t) = 0.2$.

Next, we consider the following time-periodic nutrient input with some period $T > 0$:

$$\lambda(t) = \begin{cases} 0.5, & 0 \leq t < \frac{T}{2}, \\ 0, & \frac{T}{2} \leq t < T, \end{cases} \quad (49)$$

with natural periodic extension to \mathbb{R}^+ . In the first semi-period, the input of nutrient is relatively sufficient while in the second semi-period period, there is no nutrient input. With this periodic nutrient input, the total density also tends to be periodic, tumor grows in each semi-period with nutrient input, while during the starvation semi-period, population decays. The graphs of total density n at NT (the end of a starvation semi-period) and $NT + \frac{1}{2}T$ (the end of a semi-period with nutrients input), for some $N \in \mathbb{N}$, with the period $T = 20$ are shown in Figure 10a. Here we choose three different $k_{1,\max}$ in three line-styles: solid line for $k_{1,\max} = 0$, dashed line for $k_{1,\max} = 2$ and dash-dot line for $k_{1,\max} = 8$. Each line-style has two curves: the higher one is plotted at $NT + \frac{1}{2}T$, i.e., after a semi-period with nutrient input, and the lower one is plotted at NT , i.e., after a starvation semi-period. After a starvation semi-period, the total density is low but the width of “proliferating rim” is the same as at the end of a semi-period with nutrient input. If we consider a longer period $T = 40$ (Figure 10b), the width of tumor after a semi-period with nutrient input is longer, but the density after a starvation period is lower, in particular, one can see when $k_{1,\max} = 0$ the population at the end of a starvation semi-period is so low that it can hardly be observed compared to the population at the end of a semi-period with nutrient input.

Finally, we look at how the total population oscillates with such periodic nutrient input. In Figure 11a, for all three choices of $k_{1,\max}$, the total population $\int_{\Omega} n(x,t)dx$ oscillates periodically with similar amplitudes under the periodic nutrients input. If we extend the model to consider the following logistic type growth rates:

$$G(c,n) = g(M - n)c - \delta, \quad (50)$$

where $M > 0$ is the carrying capacity and $g > 0$. Simulations with (50) (Figure 11b) show that population with autophagy has a smaller oscillation amplitude than that without autophagy, similar to that in [18].

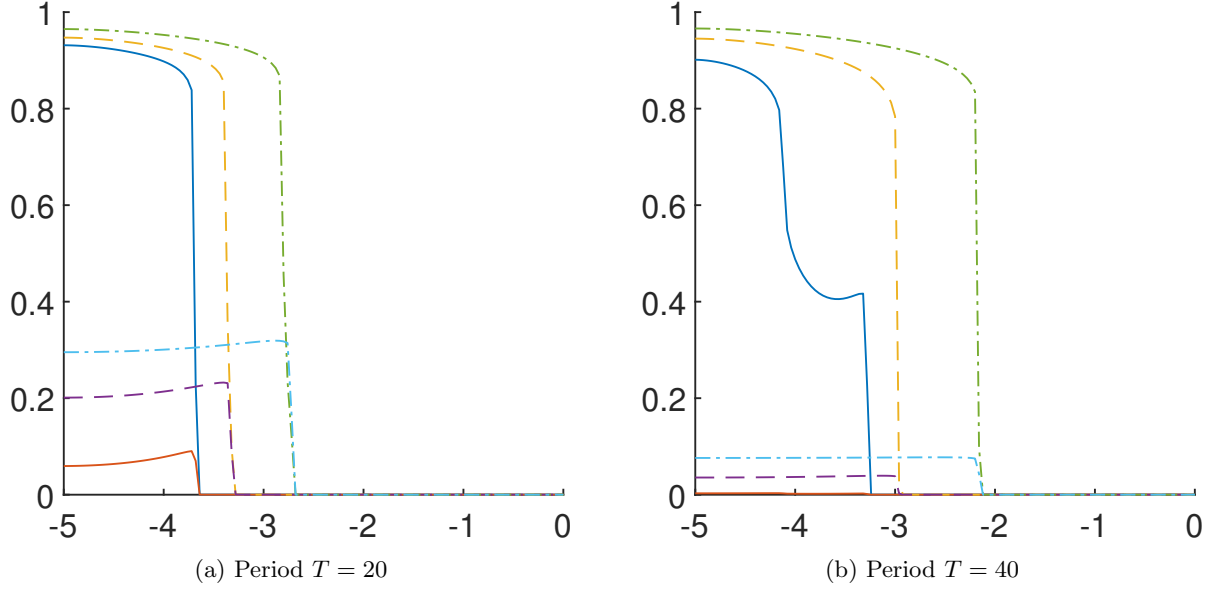


Figure 10: Plots of the total density n with a periodic nutrient input at the beginning and at the end of the starvation semi-period. Blue solid line: $k_{1,\max} = 0$ at $NT + \frac{1}{2}T$ ($N \in \mathbb{N}$). Orange solid line: $k_{1,\max} = 0$ at NT . Yellow dashed line: $k_{1,\max} = 2$ at $NT + \frac{1}{2}T$. Purple dashed line: $k_{1,\max} = 2$ at NT . Green dash-dot line: $k_{1,\max} = 8$ at $NT + \frac{1}{2}T$. Light blue dash-dot line: $k_{1,\max} = 8$ at NT . Other parameters: $\gamma = 40$, $a = 0.5$, $\delta = 0.5$, $D = 0.1$, $k_{2,\max} = 1$, $\omega = 0.5$. Nutrient input: (49) with $T = 20, 40$.

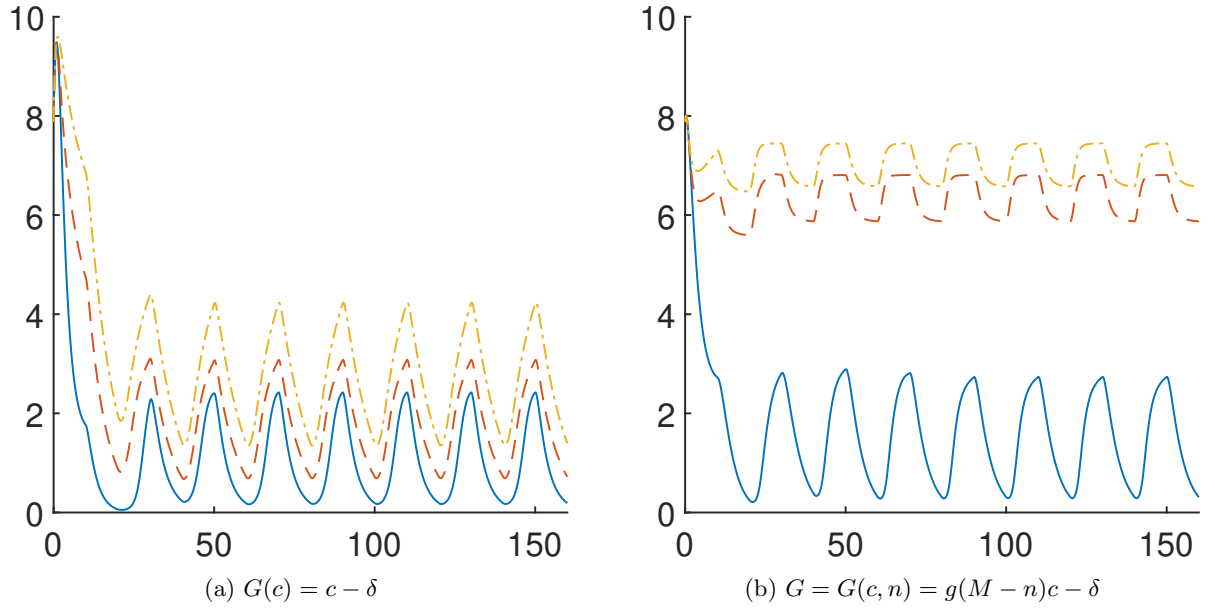


Figure 11: Evolution of the total population with a time-periodic nutrient input. (a): linear growth rate (46). (b): logistic growth rate (50). Solid line: $k_{1,\max} = 0$. Dashed line: $k_{1,\max} = 2$. Dash-dot line: $k_{1,\max} = 8$. Parameters for logistic growth rates: $g = 2$, $M = 1.2$. Other parameters: $\gamma = 40$, $a = 0.5$, $\delta = 0.5$, $D = 0.1$, $k_{2,\max} = 1$, $\omega = 0.5$, $N_1 = N_2 = 4$.

Acknowledgements

This work has been partially supported by Beijing Academy of Artificial Intelligence (BAAI). X. Dou is partially supported by the elite undergraduate training program of School of Mathematical Sciences in Peking University. J. Liu is partially supported by National Science Foundation (NSF) under award DMS-1812573. Z. Zhou is supported by

NSFC grant No. 11801016. The authors thank Jinzhi Lei and Benoît Perthame for helpful discussions.

Appendix A The proof of Proposition 2

Proof of Proposition 2. Since ∇p is Lipschitz in space thanks to p is C^2 in space by Assumption 2, we could apply Picard's theorem to obtain the uniqueness and local existence.

Note that when $y \in \partial\Omega(0)$ the ODE is exactly the evolution of boundary in Assumption 2. Thus it is well-defined and by our definition $\partial\Omega(t) = X_{t,0}(\partial\Omega(0))$.

Then we could obtain $x(t, y) \in \Omega(t)$ (if the flow exists for time t) for $y \in \Omega(0)$. Combine this with continuity of ∇p , we could extend the local solution to get the existence in $[0, T)$.

It remains to show $X_{t,0}(\Omega(0)) = \Omega(t)$. We have obtained $X_{t,0}(\Omega(0)) \subseteq \Omega(t)$, it remains to prove that for all $x \in \Omega(t)$, there exists $y \in \Omega(0)$ such that $x = X_{t,0}(y)$. This can be obtained by solving flow map (22) backward and apply the same argument in the first part of proof. \square

Appendix B Numerical scheme for the compressible model

We adapt the numerical scheme in [23] for the compressible cell density model (5) and (45). In this section we present the details of the scheme. For properties and analysis on the scheme we refer to [23].

The main difficulty is the nonlinearity in (6) with high γ . In the projection and correlation framework of [24], they introduce the velocity field \mathbf{u} :

$$\mathbf{u} := -\nabla p.$$

and solve the equation for \mathbf{u} ,

$$\frac{\partial \mathbf{u}}{\partial t} = \gamma \nabla (n^{\gamma-2} (\nabla \cdot (n \mathbf{u}) - n_1 G_1(c) - n_2 G_2(c))). \quad (51)$$

Here we use the shorthand notation $G_1(c) = G(c)$, $G_2(c) = G(c) - D$.

We first present the scheme on the system with Neumann boundary condition (45). And we describe the update from (u^j, n_1^j, n_2^j, c^j) to $(u^{j+1}, n_1^{j+1}, n_2^{j+1}, c^{j+1})$ in one-dimension.

Consider the domain $\Omega = [a, b]$. $\Delta x = \frac{b-a}{N}$ be the spatial mesh size, and the grid points are

$$x_i = a + i\Delta x, \quad x_{i+\frac{1}{2}} = a + (i + \frac{1}{2})\Delta x,$$

in regular grid and staggered grid, respectively. As in [23] the regular grid is for total density n and the staggered grid is for the velocity field u .

First we solve the equation for velocity field u (51) to get u^* :

$$\begin{aligned} \frac{u_{i+1/2}^{j*} - u_{i+1/2}^j}{\Delta t} = \frac{\gamma}{\Delta x} & \left\{ \left((n_{i+1}^j)^{\gamma-2} \left(\frac{n_{i+3/2}^j u_{i+3/2}^{j*} - n_{i+1/2}^j u_{i+1/2}^{j*}}{\Delta x} - n_{1,i+1}^j G_{1,i+1}^j - n_{2,i+1}^j G_{2,i+1}^j \right) \right) \right. \\ & \left. - \left((n_i^j)^{\gamma-2} \left(\frac{n_{i+1/2}^j u_{i+1/2}^{j*} - n_{i-1/2}^j u_{i-1/2}^{j*}}{\Delta x} - n_{1,i}^j G_{1,i}^j - n_{2,i}^j G_{2,i}^j \right) \right) \right\}, \end{aligned} \quad (52)$$

Here $n_{1,i}, n_{2,i}$ are the spatial discretization for n_1, n_2 . And $G_{1,i}^j = G_1(c_i^j)$, $G_{2,i}^j = G_2(c_i^j)$. The value of n on the staggered grid is approximated by

$$n_{i+\frac{1}{2}}^j = \frac{n_i^j + n_{i+1}^j}{2}.$$

The no-flux boundary condition is treated as

$$n_{\frac{1}{2}}^j u_{\frac{1}{2}}^j = n_{N-\frac{1}{2}}^j u_{N-\frac{1}{2}}^j = 0. \quad (53)$$

With u^* obtained, the two equations for n_1, n_2 are discretized by a central scheme, and we treat the reaction term semi-implicitly.

$$\begin{aligned} \frac{n_{1,i}^{j+1} - n_{1,i}^j}{\Delta t} + \frac{F_{1,i+1/2}^j - F_{1,i-1/2}^j}{\Delta x} &= G_{1,i}^j n_{1,i}^{j+1} - K_{1,i}^j n_{1,i}^{j+1} + K_{2,i}^j n_{2,i}^{j+1} \\ \frac{n_{2,i}^{j+1} - n_{2,i}^j}{\Delta t} + \frac{F_{2,i+1/2}^j - F_{2,i-1/2}^j}{\Delta x} &= G_{2,i}^j n_{2,i}^{j+1} + K_{1,i}^j n_{1,i}^{j+1} - K_{2,i}^j n_{2,i}^{j+1}. \end{aligned} \quad (54)$$

Here $K_{1,i}^j = K_1(c_i^j)$, $K_{2,i}^j = K_2(c_i^j)$.

Now we describe how to compute the flux F_1, F_2 . For clarity we omit the dependence on the specific kind of cells and, with a bit abuse of notation, use n_i^j instead of $n_{1,i}^j, n_{2,i}^j$. When computing F_1 , n_i^j in the following should be substituted by $n_{1,i}^j$. Similarly when computing F_2 , n_i^j should be substituted by $n_{2,i}^j$.

$$F_{i\pm 1/2}^j = \frac{1}{2} \left[n^{Lj} u^{j*} + n^{Rj} u^{j*} - |u^{j*}| (n^{Rj} - n^{Lj}) \right]_{i\pm 1/2}$$

Here the edge values $n_{i\pm 1/2}^{L/Rj}$ are defined as follows:

$$n_{i+1/2}^{Lj} = n_i^j + \frac{\Delta x}{2} (\partial_x n)_i^j, \quad n_{i+1/2}^{Rj} = n_{i+1}^j - \frac{\Delta x}{2} (\partial_x n)_{i+1}^j,$$

where $(\partial_x n)_i^j$ is given by

$$(\partial_x n)_i^j = \begin{cases} \min\left\{\frac{n_{i+1}^j - n_i^j}{\Delta x}, \frac{n_{i+1}^j - n_{i-1}^j}{2\Delta x}, \frac{n_i^j - n_{i-1}^j}{\Delta x}\right\}, & \text{if all are positive,} \\ \max\left\{\frac{n_{i+1}^j - n_i^j}{\Delta x}, \frac{n_{i+1}^j - n_{i-1}^j}{2\Delta x}, \frac{n_i^j - n_{i-1}^j}{\Delta x}\right\}, & \text{if all are negative,} \\ 0, & \text{otherwise.} \end{cases}$$

After obtaining $n_{1,i}^{j+1}$ and $n_{2,i}^{j+1}$, we compute the new total density n and new velocity field u :

$$n_i^{j+1} = n_{1,i}^{j+1} + n_{2,i}^{j+1}, \quad u_{i+1/2}^{j+1} = -\frac{\gamma}{\gamma-1} \frac{(n_{i+1}^{j+1})^\gamma - (n_i^{j+1})^\gamma}{\Delta x}. \quad (55)$$

Finally, for the concentration of nutrients c , since we simulate the linear case $\psi(c) = c$, we use standard finite difference method for the diffusion equation with Neumann boundary condition:

$$\begin{aligned} \frac{c_i^{j+1} - c_i^j}{\Delta t} - \frac{c_{i+1}^{j+1} - 2c_i^{j+1} + c_{i-1}^{j+1}}{(\Delta x)^2} + c_i^{j+1} n_i^{j+1} &= a n_{2,i}^{j+1}, \\ \frac{c_1^{j+1} - c_0^{j+1}}{\Delta x} = \frac{c_{N-1}^{j+1} - c_N^{j+1}}{\Delta x} &= \lambda^{j+1} = \lambda((j+1)\Delta t). \end{aligned} \quad (56)$$

For the Cauchy problem, we reduce it to the Neumann problem by choosing the computation domain larger than the support of n . In simulation we track the support of n and dynamically enlarge the computation domain such that it is much larger than the support of n . In the support of n we solve the equation of c (8) by standard finite difference method.

References

- [1] Michiel Bertsch, Roberta Dal Passo, and Masayasu Mimura. A free boundary problem arising in a simplified tumour growth model of contact inhibition. *Interfaces and Free Boundaries*, 12(2):235–250, 2010.
- [2] Michiel Bertsch, Danielle Hilhorst, Hirofumi Izuhara, and Masayasu Mimura. A nonlinear parabolic-hyperbolic system for contact inhibition of cell-growth. *Differ. Equ. Appl*, 4(1):137–157, 2012.
- [3] Didier Bresch, Thierry Colin, Emmanuel Grenier, Benjamin Ribba, and Olivier Saut. Computational modeling of solid tumor growth: The avascular stage. *SIAM Journal on Scientific Computing*, 32(4):2321–2344, 2010.
- [4] Federica Bubba, Benoît Perthame, Camille Pouchol, and Markus Schmidtchen. Hele–shaw limit for a system of two reaction-(cross-) diffusion equations for living tissues. *Archive for Rational Mechanics and Analysis*, pages 1–32, 2019.
- [5] José A Carrillo, Simone Fagioli, Filippo Santambrogio, and Markus Schmidtchen. Splitting schemes and segregation in reaction cross-diffusion systems. *SIAM Journal on Mathematical Analysis*, 50(5):5695–5718, 2018.
- [6] Xinfu Chen, Shangbin Cui, and Avner Friedman. A hyperbolic free boundary problem modeling tumor growth: Asymptotic behavior. *Transactions of the American Mathematical Society*, 357(12):4771–4804, 2005.
- [7] Xinfu Chen and Avner Friedman. A free boundary problem for an elliptic-hyperbolic system: An application to tumor growth. *Siam Journal on Mathematical Analysis*, 35(4):974–986, 2003.
- [8] Shangbin Cui. Asymptotic stability of the stationary solution for a hyperbolic free boundary problem modeling tumor growth. *Siam Journal on Mathematical Analysis*, 40(4):1692–1724, 2008.

- [9] Shangbin Cui and Avner Friedman. Analysis of a mathematical model of the growth of necrotic tumors. *Journal of Mathematical Analysis and Applications*, 255(2):636–677, 2001.
- [10] Shangbin Cui and Avner Friedman. A hyperbolic free boundary problem modeling tumor growth. *Interfaces and Free Boundaries*, 5(2):159–182, 2003.
- [11] Shangbin Cui and Xuemei Wei. Global existence for a parabolic-hyperbolic free boundary problem modelling tumor growth. *Acta Mathematicae Applicatae Sinica*, 21(4):597–614, 2005.
- [12] Noemi David and Benoît Perthame. Free boundary limit of tumor growth model with nutrient. working paper or preprint, hal-02515263, March 2020.
- [13] Pierre Degond, Sophie Hecht, and Nicolas Vauchelet. Incompressible limit of a continuum model of tissue growth for two cell populations. *Networks and Heterogeneous Media*, 15(1):57–85, 2020.
- [14] Avner Friedman. A hierarchy of cancer models and their mathematical challenges. *Discrete and Continuous Dynamical Systems Series B*, 4(1):147–160, 2004.
- [15] Avner Friedman. Mathematical analysis and challenges arising from models of tumor growth. *Mathematical Models and Methods in Applied Sciences*, 17(supp01):1751–1772, 2007.
- [16] Francisco Guillengonzalez and Juan Vicente Gutierrezsantacreu. From a cell model with active motion to a heleshaw-like system: a numerical approach. *Numerische Mathematik*, 143(1):107–137, 2019.
- [17] Piotr Gwiazda, Benoît Perthame, and Agnieszka Świerczewska-Gwiazda. A two-species hyperbolic–parabolic model of tissue growth. *Communications in Partial Differential Equations*, 44(12):1605–1618, 2019.
- [18] Huiqin Jin and Jinzhi Lei. A mathematical model of cell population dynamics with autophagy response to starvation. *Mathematical biosciences*, 258:1–10, 2014.
- [19] Rekha Khandia, Maryam Dadar, Ashok Munjal, Kuldeep Dhama, Kumaragurubaran Karthik, Ruchi Tiwari, Mohd Yattoo, Hafiz Iqbal, Karam Pal Singh, Sunil K Joshi, et al. A comprehensive review of autophagy and its various roles in infectious, non-infectious, and lifestyle diseases: Current knowledge and prospects for disease prevention, novel drug design, and therapy. *Cells*, 8(7):674, 2019.
- [20] Daniel J Klionsky. Autophagy: from phenomenology to molecular understanding in less than a decade. *Nature reviews Molecular cell biology*, 8(11):931–937, 2007.
- [21] Beth Levine. Autophagy and cancer. *Nature*, 446(7137):745–747, 2007.
- [22] Jean M Mulcahy Levy and Andrew Thorburn. Autophagy in cancer: Moving from understanding mechanism to improving therapy responses in patients. *Cell Death & Differentiation*, pages 1–15, 2019.
- [23] Jian-Guo Liu, Min Tang, Li Wang, and Zhennan Zhou. An accurate front capturing scheme for tumor growth models with a free boundary limit. *Journal of Computational Physics*, 364:73–94, 2018.
- [24] Jian-Guo Liu, Min Tang, Li Wang, and Zhennan Zhou. Analysis and computation of some tumor growth models with nutrient: From cell density models to free boundary dynamics. *Discrete and Continuous Dynamical Systems-series B*, 24(7):3011–3035, 2019.
- [25] Jianguo Liu, Min Tang, Li Wang, and Zhennan Zhou. Towards understanding the boundary propagation speeds in tumor growth models. *arXiv: Analysis of PDEs*, 2019.
- [26] Tommaso Lorenzi, Alexander Lorz, and Benoît Perthame. On interfaces between cell populations with different mobilities. *Kinetic and Related Models*, 10(1):299–311, 2016.
- [27] Séverine Lorin, Ahmed Hamai, Maryam Mehrpour, and Patrice Codogno. Autophagy regulation and its role in cancer. In *Seminars in cancer biology*, volume 23, pages 361–379. Elsevier, 2013.
- [28] John Lowengrub, Hermann B Frieboes, Fang Jin, Yaoli Chuang, Xiangrong Li, Paul Macklin, Steven M Wise, and Vittorio Cristini. Nonlinear modelling of cancer: bridging the gap between cells and tumours. *Nonlinearity*, 23(1), 2010.
- [29] Antoine Mellet, Benoît Perthame, and Fernando Quiros. A hele–shaw problem for tumor growth. *Journal of Functional Analysis*, 273(10):3061–3093, 2017.
- [30] Athanasios Metaxakis, Christina Ploumi, and Nektarios Tavernarakis. Autophagy in age-associated neurodegeneration. *Cells*, 7(5):37, 2018.

- [31] Noboru Mizushima and Masaaki Komatsu. Autophagy: renovation of cells and tissues. *Cell*, 147(4):728–741, 2011.
- [32] Hideaki Morishita and Noboru Mizushima. Diverse cellular roles of autophagy. *Annual review of cell and developmental biology*, 35:453–475, 2019.
- [33] Benoît Perthame. Some mathematical models of tumor growth. 2015. https://www.ljll.math.upmc.fr/perthame/cours_M2.pdf.
- [34] Benoît Perthame, Fernando Quirós, and Juan Luis Vázquez. The hele–shaw asymptotics for mechanical models of tumor growth. *Archive for Rational Mechanics and Analysis*, 212(1):93–127, 2014.
- [35] Benoît Perthame, Min Tang, and Nicolas Vauchelet. Traveling wave solution of the hele–shaw model of tumor growth with nutrient. *Mathematical Models and Methods in Applied Sciences*, 24(13):2601–2626, 2014.
- [36] Graeme J Pettet, C P Please, Marcus J Tindall, and D L S McElwain. The migration of cells in multicell tumor spheroids. *Bulletin of Mathematical Biology*, 63(2):231–257, 2001.
- [37] Michelle L. Pleet, Heather Branscome, Catherine DeMarino, Daniel O. Pinto, Mohammad Asad Zadeh, Myosotis Rodriguez, Ilker Kudret Sariyer, Nazira El-Hage, and Fatah Kashanchi. Autophagy, evs, and infections: A perfect question for a perfect time. *Frontiers in Cellular and Infection Microbiology*, 8:362, 2018.
- [38] Brock C Price and Xiangsheng Xu. Global existence theorem for a model governing the motion of two cell populations. *arXiv preprint arXiv:2004.05939*, 2020.
- [39] Jonas Ranft, Markus Basan, Jens Elgeti, Jeanfrancois Joanny, Jacques Prost, and Frank Julicher. Fluidization of tissues by cell division and apoptosis. *Proceedings of the National Academy of Sciences of the United States of America*, 107(49):20863–20868, 2010.
- [40] Tiina Roose, S Jonathan Chapman, and Philip K Maini. Mathematical models of avascular tumor growth. *Siam Review*, 49(2):179–208, 2007.
- [41] Sarbari Saha, Debasna P Panigrahi, Shankargouda Patil, and Sujit K Bhutia. Autophagy in health and disease: A comprehensive review. *Biomedicine & Pharmacotherapy*, 104:485–495, 2018.
- [42] M Thumm, R Egner, B Koch, M Schlumpberger, M Straub, M Veenhuis, and DH Wolf. Isolation of autophagocytosis mutants of *saccharomyces cerevisiae*. *FEBS letters*, 349(2):275–280, 1994.
- [43] John P Ward and J R King. Mathematical modelling of avascular-tumour growth. *Mathematical Medicine and Biology-a Journal of The Ima*, 14(1):39–69, 1997.
- [44] John P Ward and J R King. Mathematical modelling of avascular-tumour growth ii: Modelling growth saturation. *Mathematical Medicine and Biology-a Journal of The Ima*, 16(2):171–211, 1999.